

**Synthesis of 5*H*-chromeno[3,4-*b*]pyridines via DABCO-catalyzed [3+3] annulation
of 3-nitro-2*H*-chromenes and allenoates**

Maria I. L. Soares,^{a,*} Clara S. B. Gomes,^{b,c} M. Conceição Oliveira,^d Joaquim Marçalo,^e Teresa M. V. D. Pinho e Melo^{a,*}

^aUniversity of Coimbra, Coimbra Chemistry Centre (CQC) and Department of Chemistry, 3004-535 Coimbra, Portugal

^bLAQV-REQUIMTE, Departamento de Química, Faculdade de Ciências e Tecnologia, Universidade NOVA de Lisboa, 2829-516 Caparica, Portugal

^cUCIBIO-REQUIMTE, Departamento de Química, Faculdade de Ciências e Tecnologia, Universidade NOVA de Lisboa, 2829-516 Caparica, Portugal

^dCentro de Química Estrutural (CQE), Instituto Superior Técnico, Universidade de Lisboa, Av. Rovisco Pais, 1049-001 Lisboa, Portugal

^eCentro de Química Estrutural (CQE), Instituto Superior Técnico, Universidade de Lisboa, 2695-066 Bobadela LRS, Portugal

*misoares@ci.uc.pt; tmelo@ci.uc.pt

Electronic Supplementary Information

Table of Contents

Copies of ^1H , ^{13}C , ^{19}F and 2D NMR Spectra for New Compounds	S2
Crystallographic Data for Compounds 3b and 4	S20
Study of the Reaction Mechanism via Mass Spectrometry Analysis	S23

Copies of ^1H , ^{13}C , ^{19}F RMN and 2D NMR Spectra for New Compounds

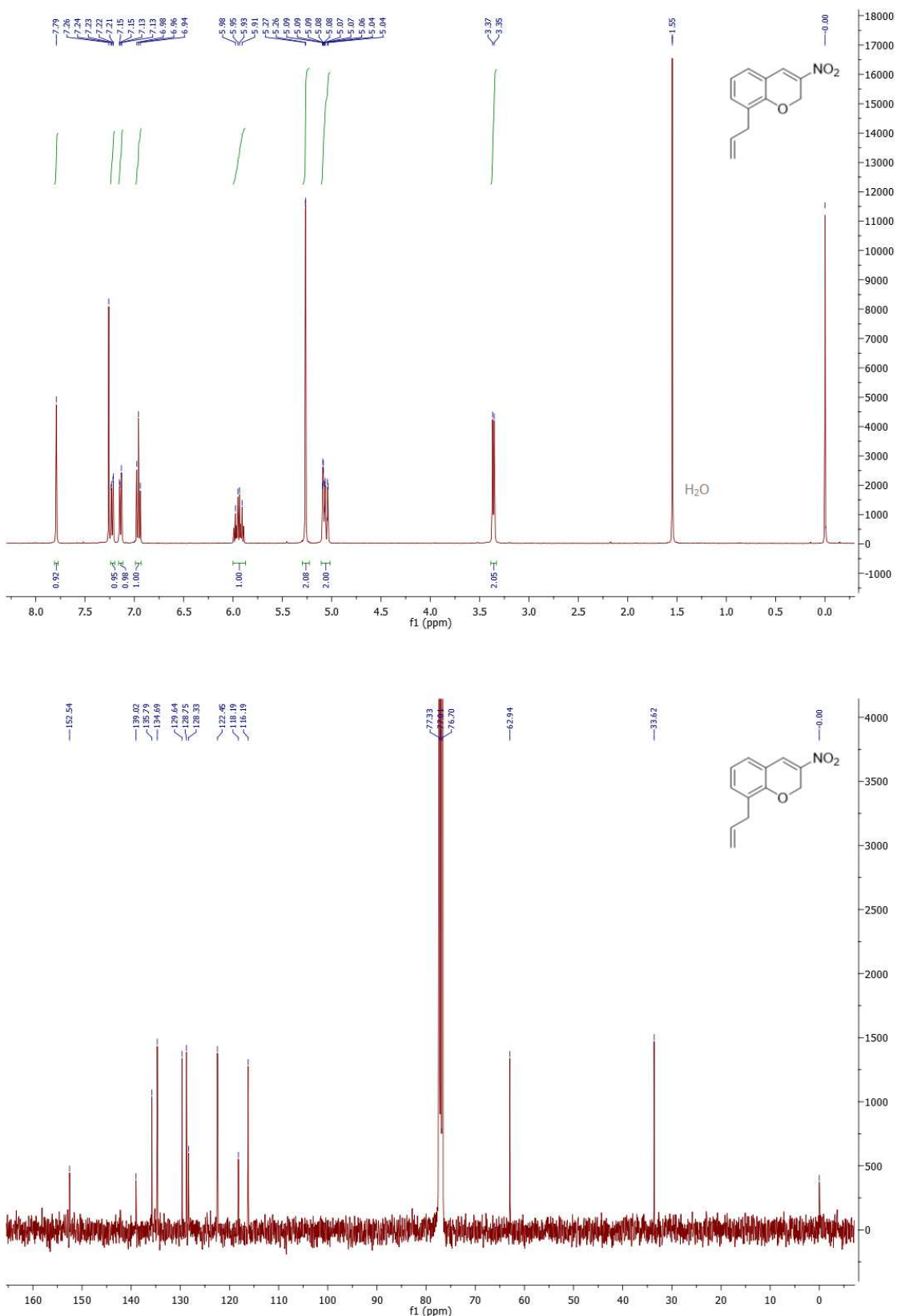


Figure S1: ^1H and ^{13}C NMR spectra of compound **1c** (CDCl_3).

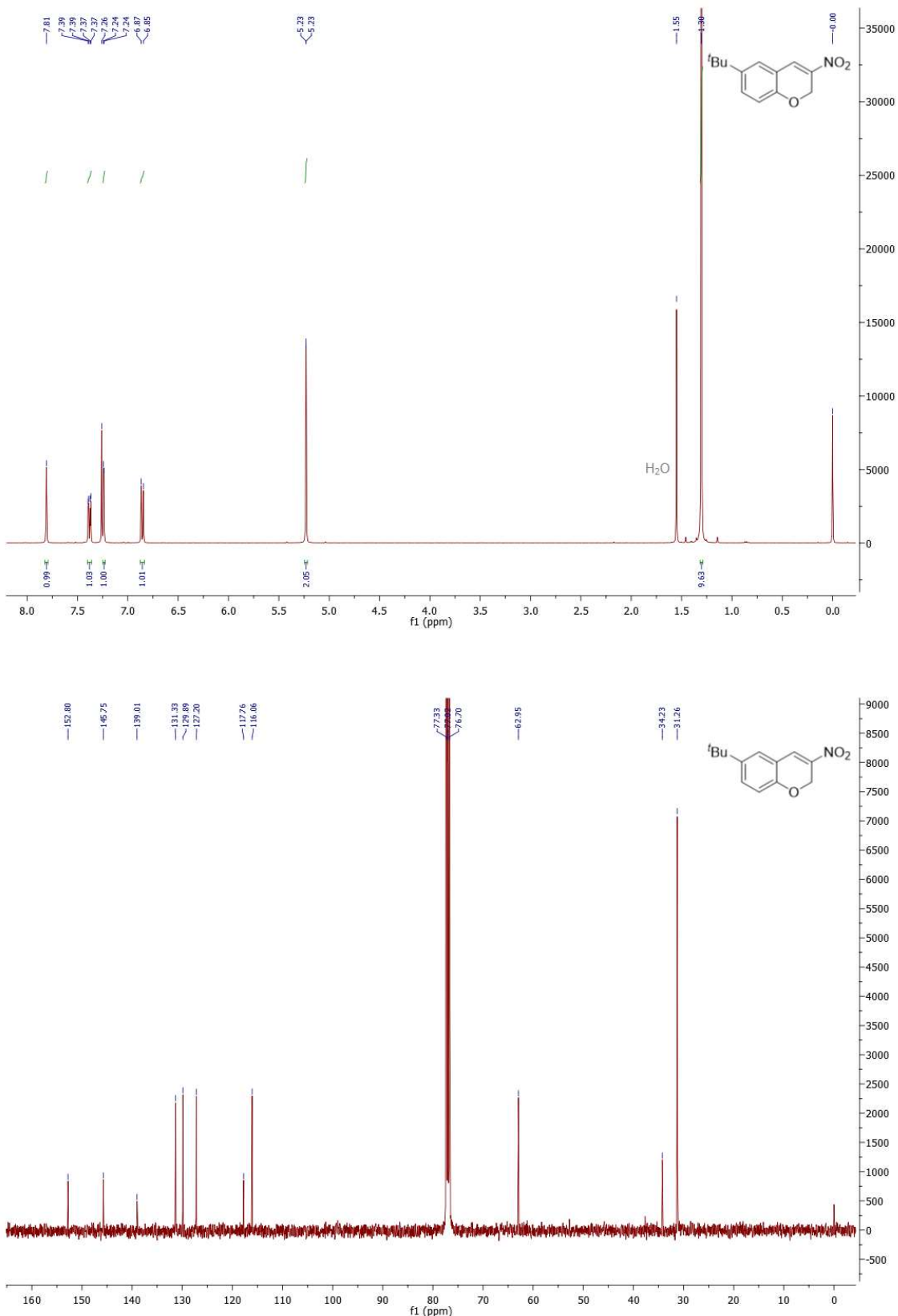


Figure S2: ^1H and ^{13}C NMR spectra of compound **1i** (CDCl_3).

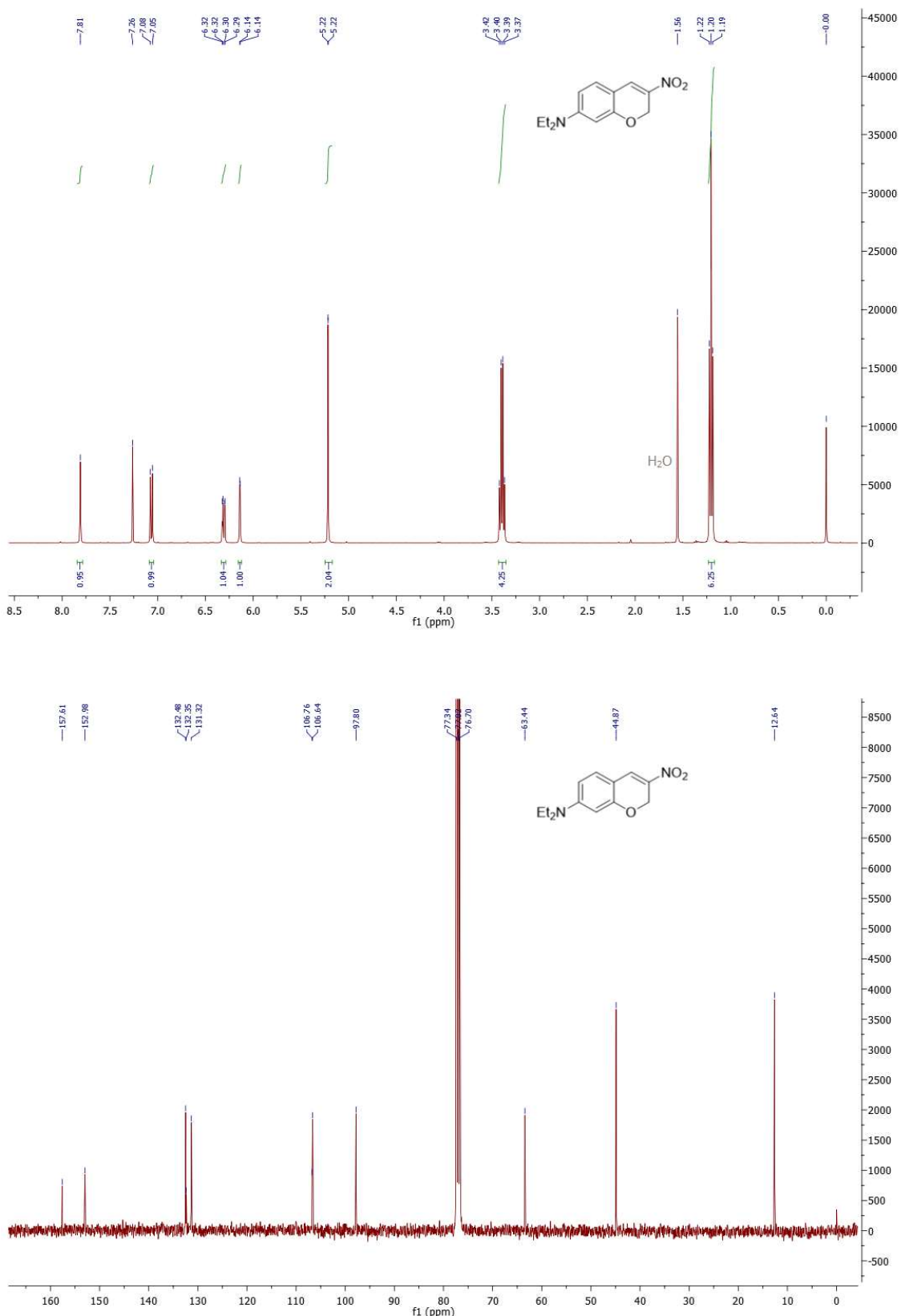


Figure S3: ^1H and ^{13}C NMR spectra of compound **1k** (CDCl_3).

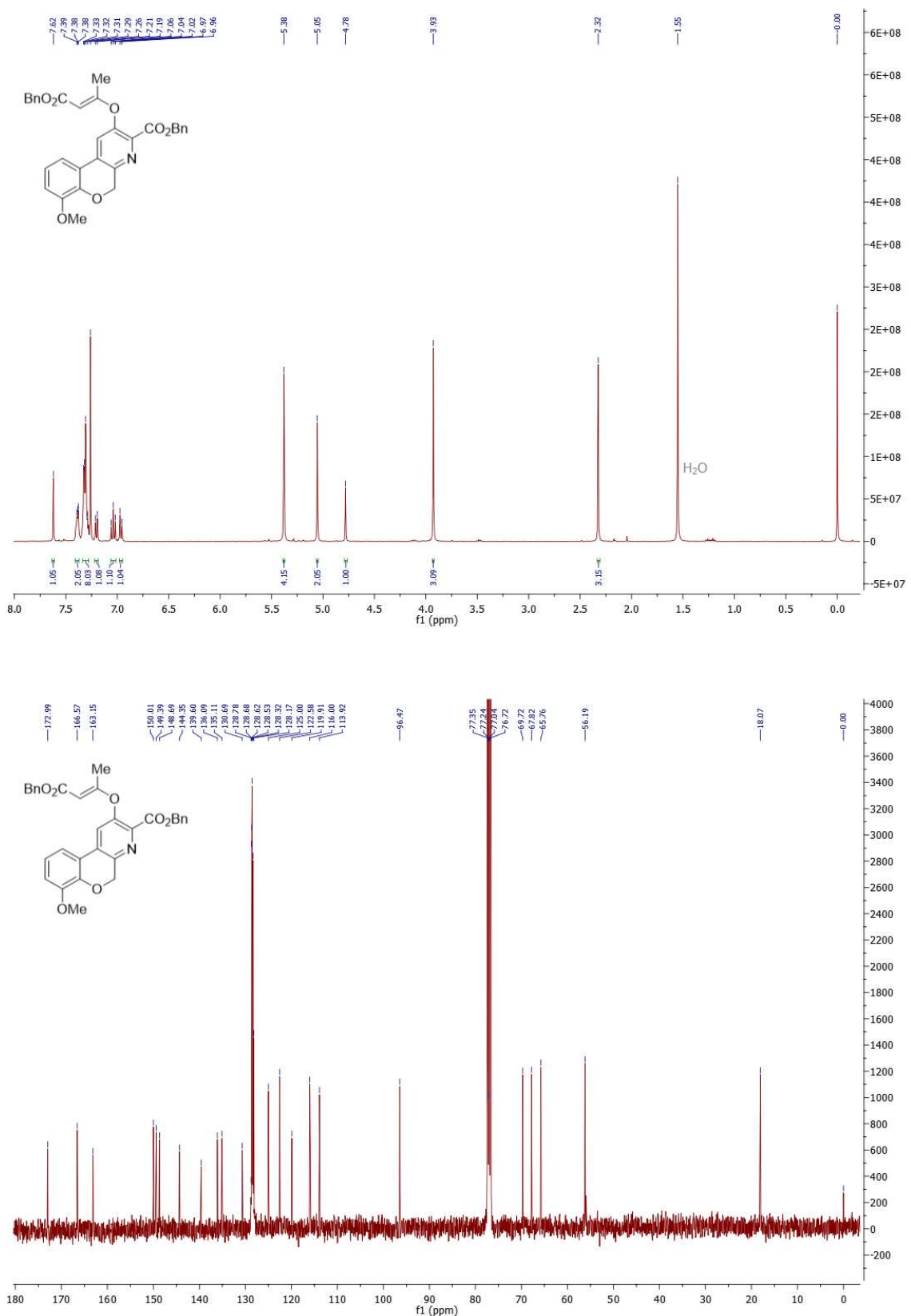


Figure S4: ^1H and ^{13}C NMR spectra of compound **3a** (CDCl_3).

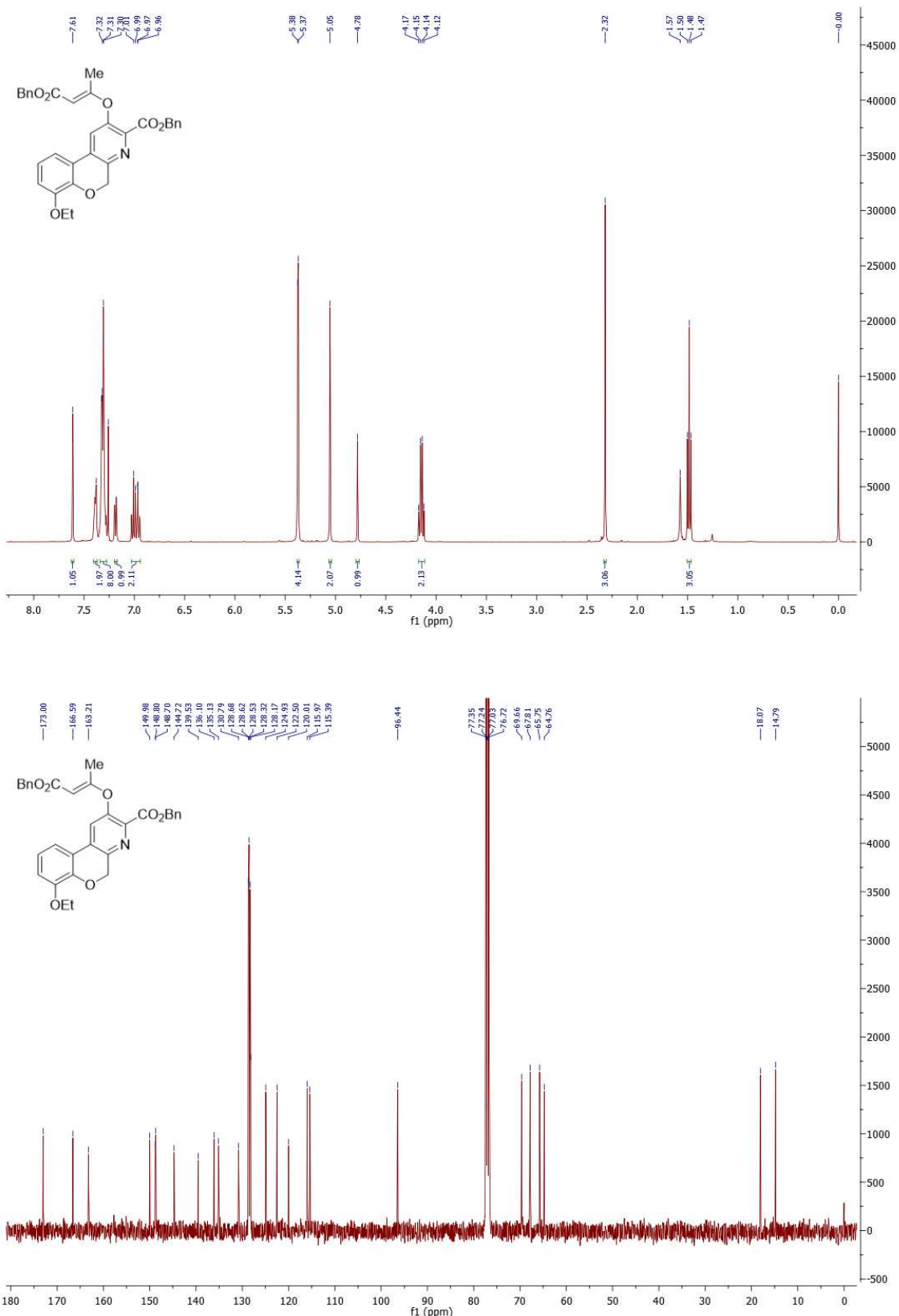


Figure S5: ^1H and ^{13}C NMR spectra of compound **3b** (CDCl_3).

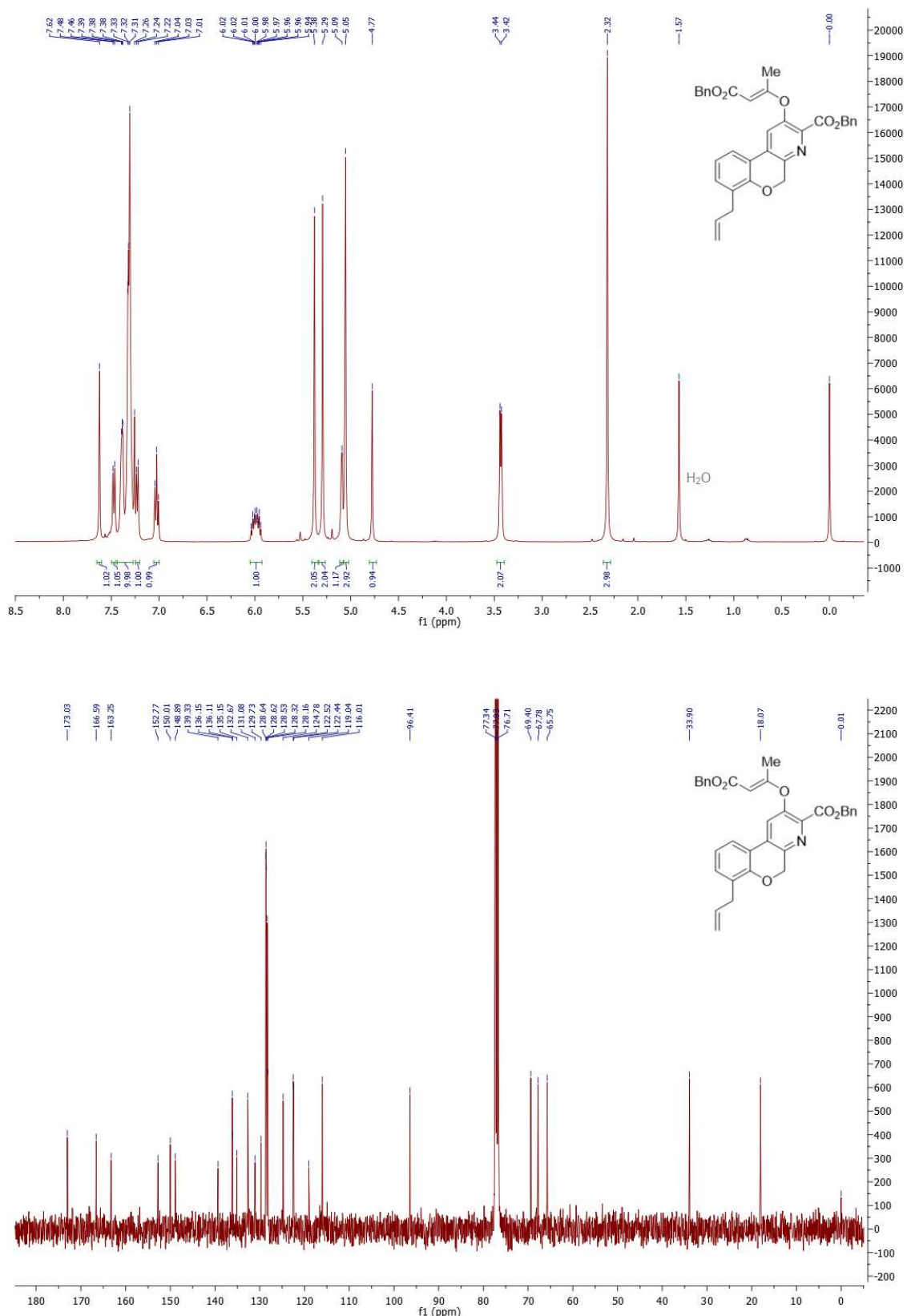


Figure S6: ^1H and ^{13}C NMR spectra of compound **3c** (CDCl_3).

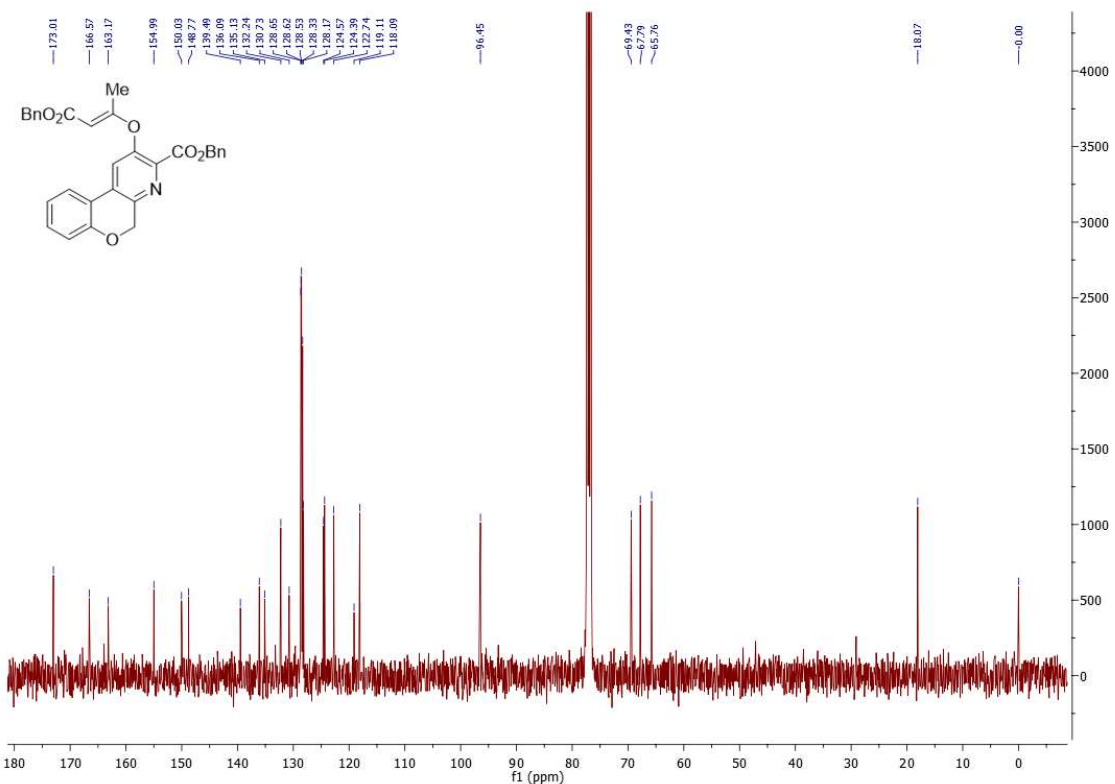
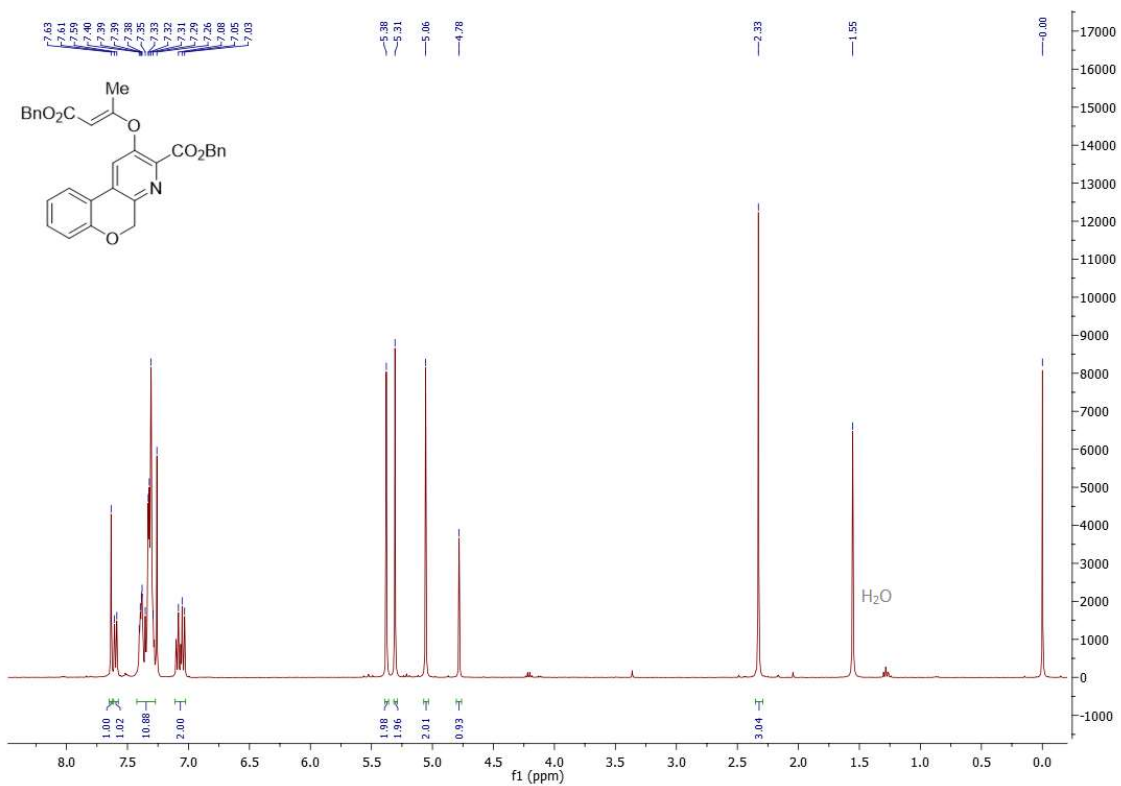
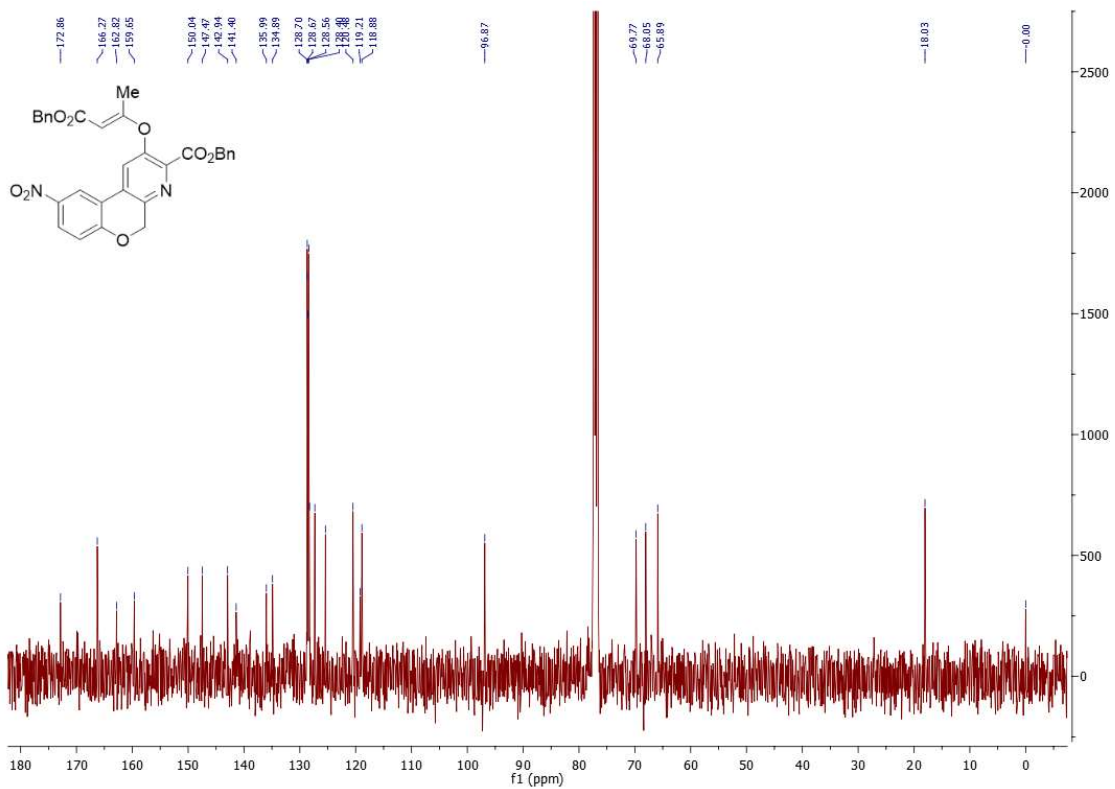
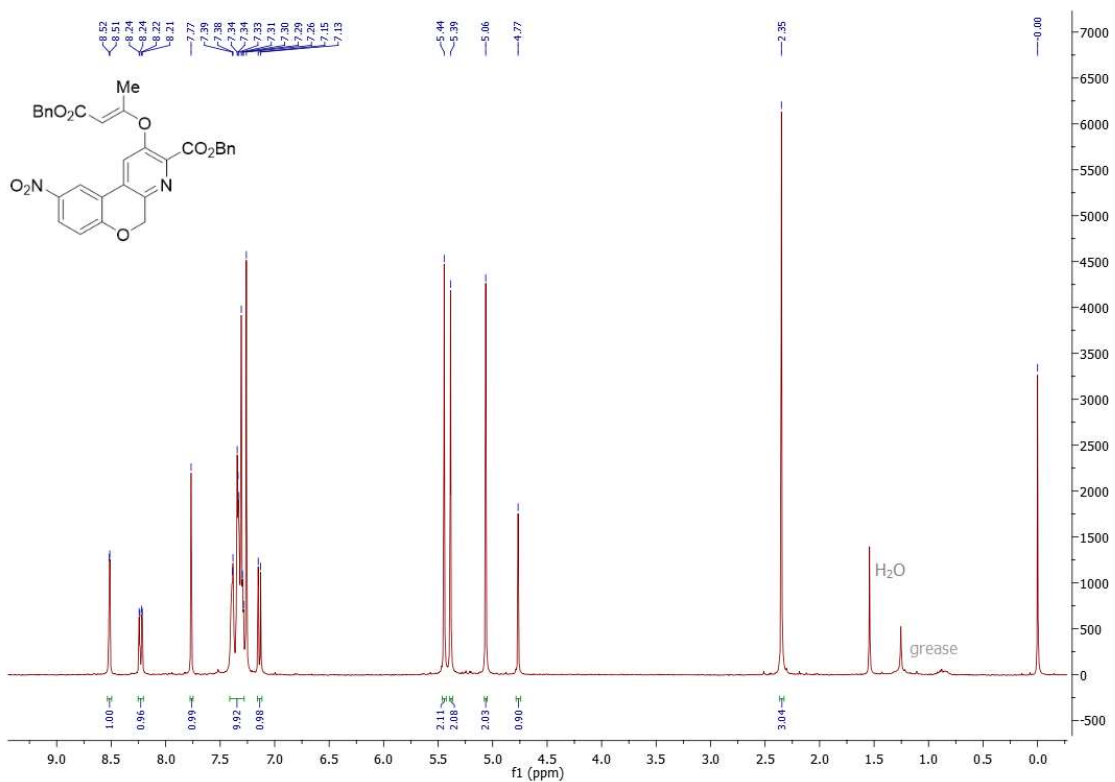


Figure S7: ^1H and ^{13}C NMR spectra of compound **3d** (CDCl_3).



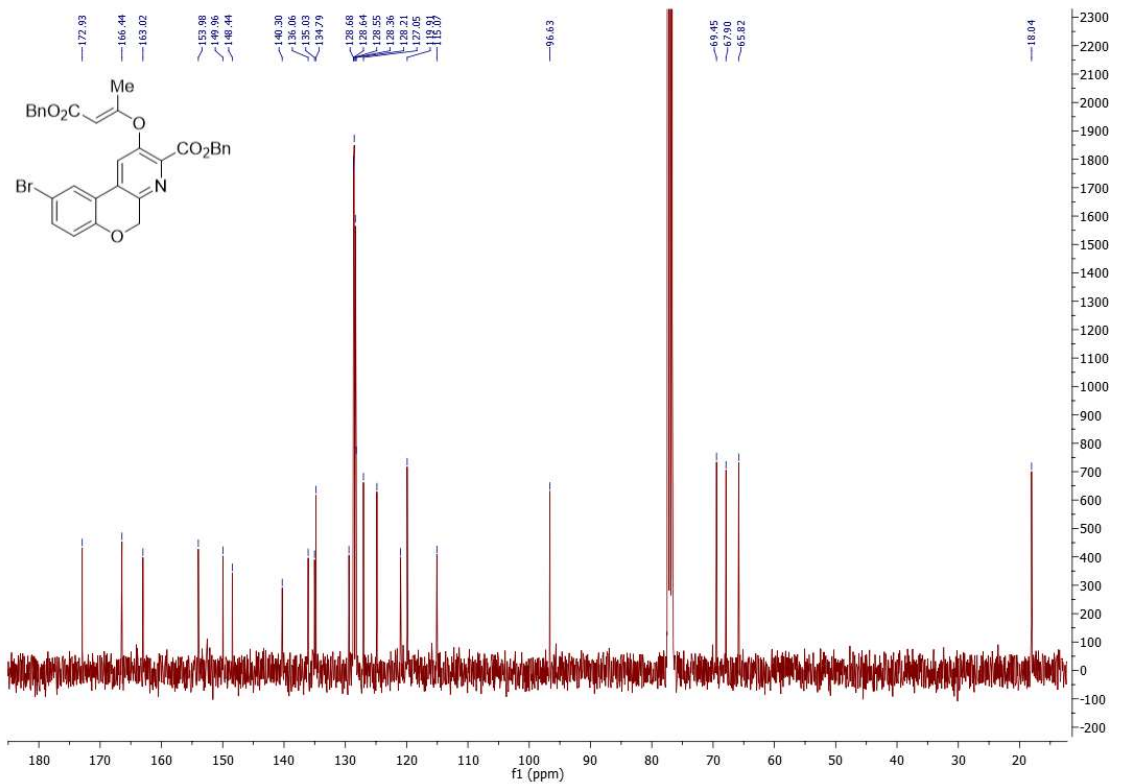
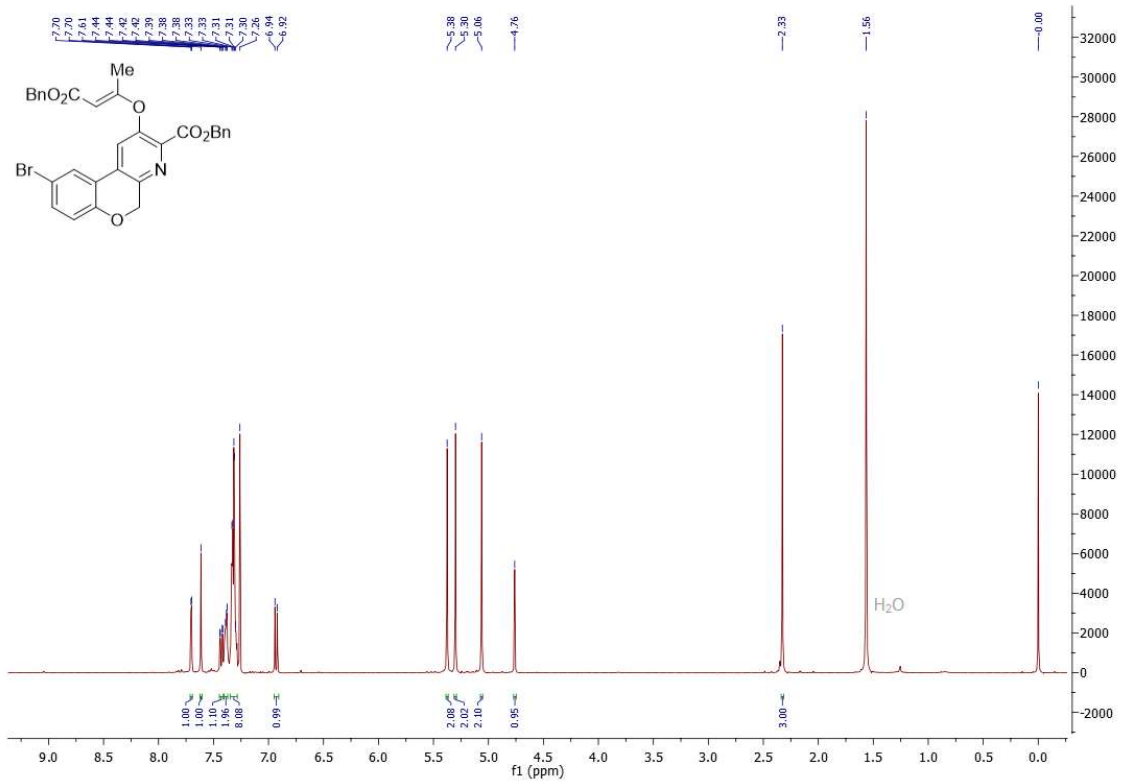


Figure S9: ^1H and ^{13}C NMR spectra of compound **3f** (CDCl_3).

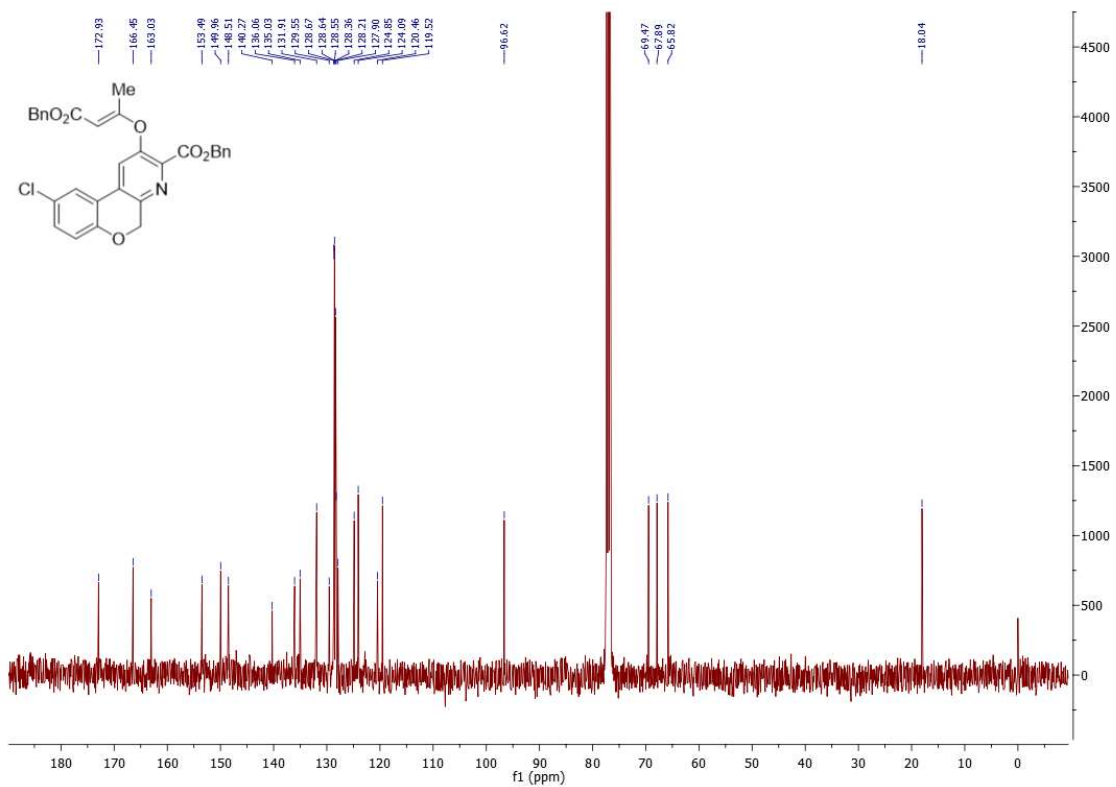
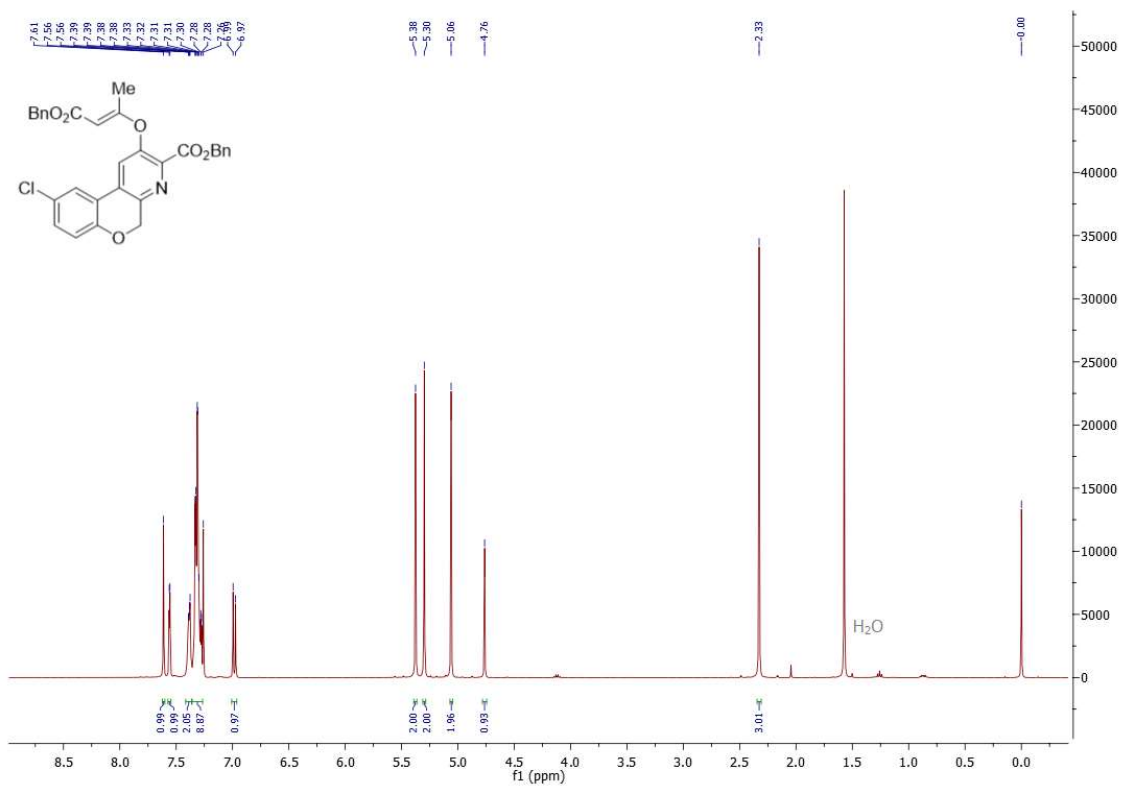


Figure S10: ^1H and ^{13}C NMR spectra of compound **3g** (CDCl_3).

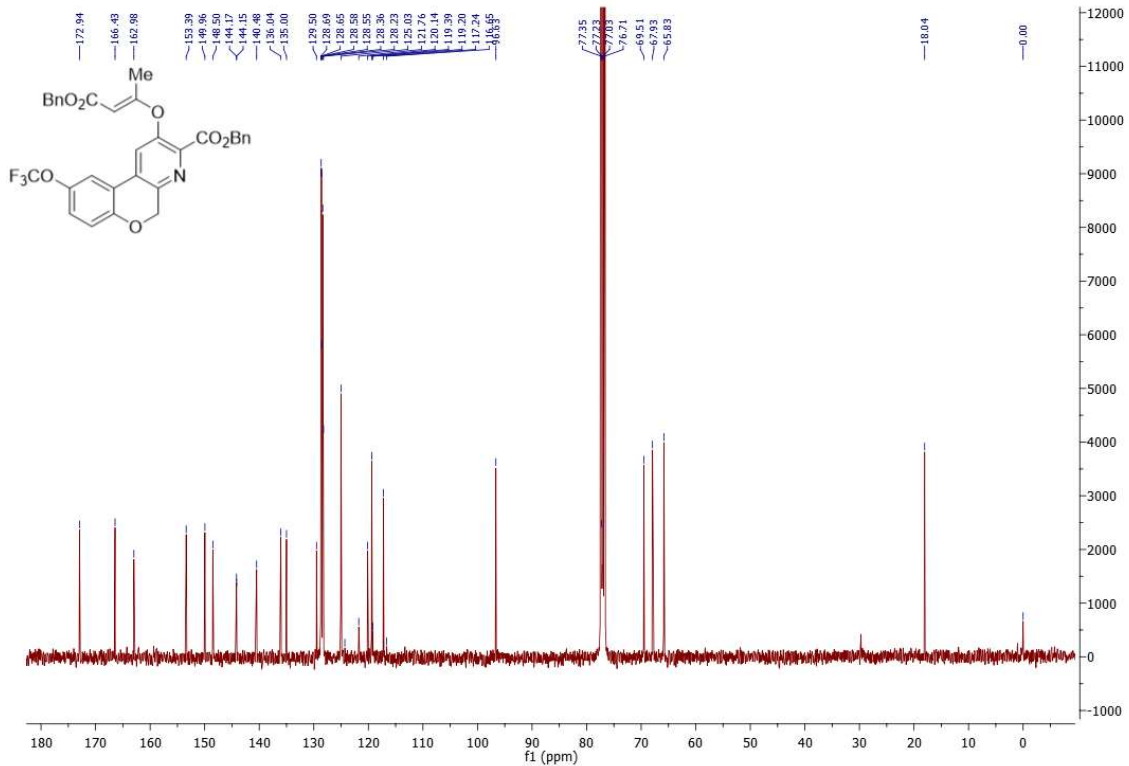
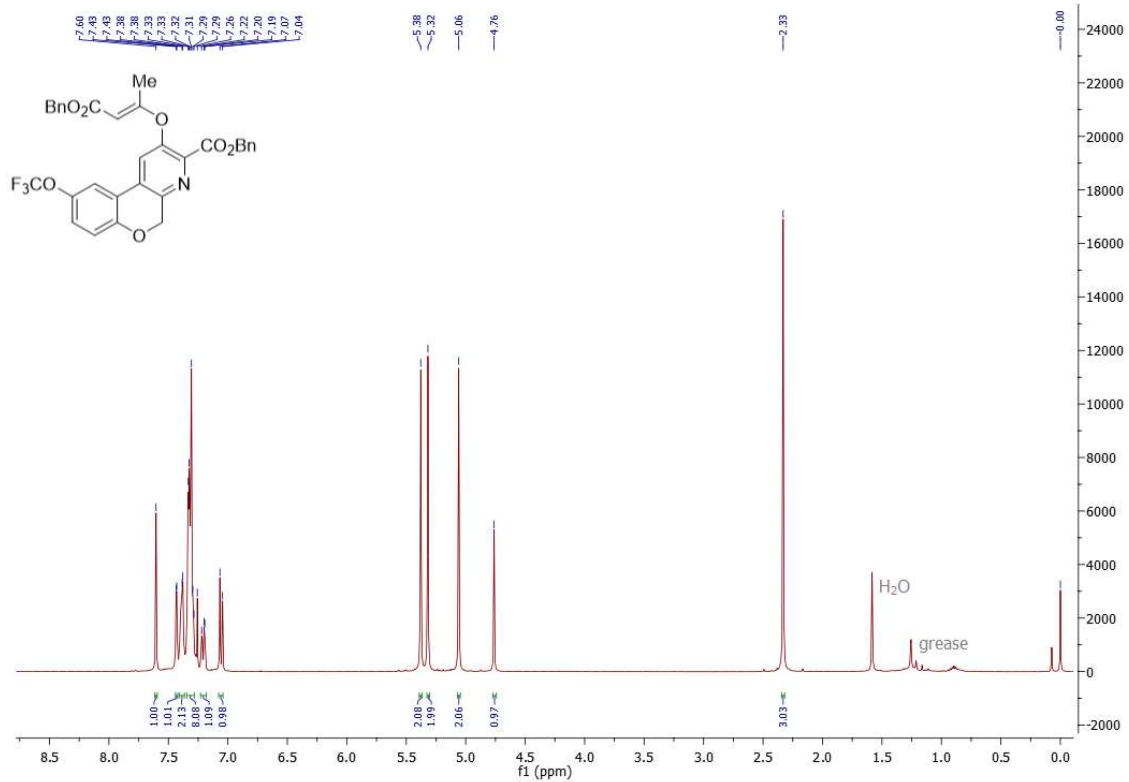


Figure S11a: ^1H and ^{13}C spectra of compound **3h** (CDCl_3).

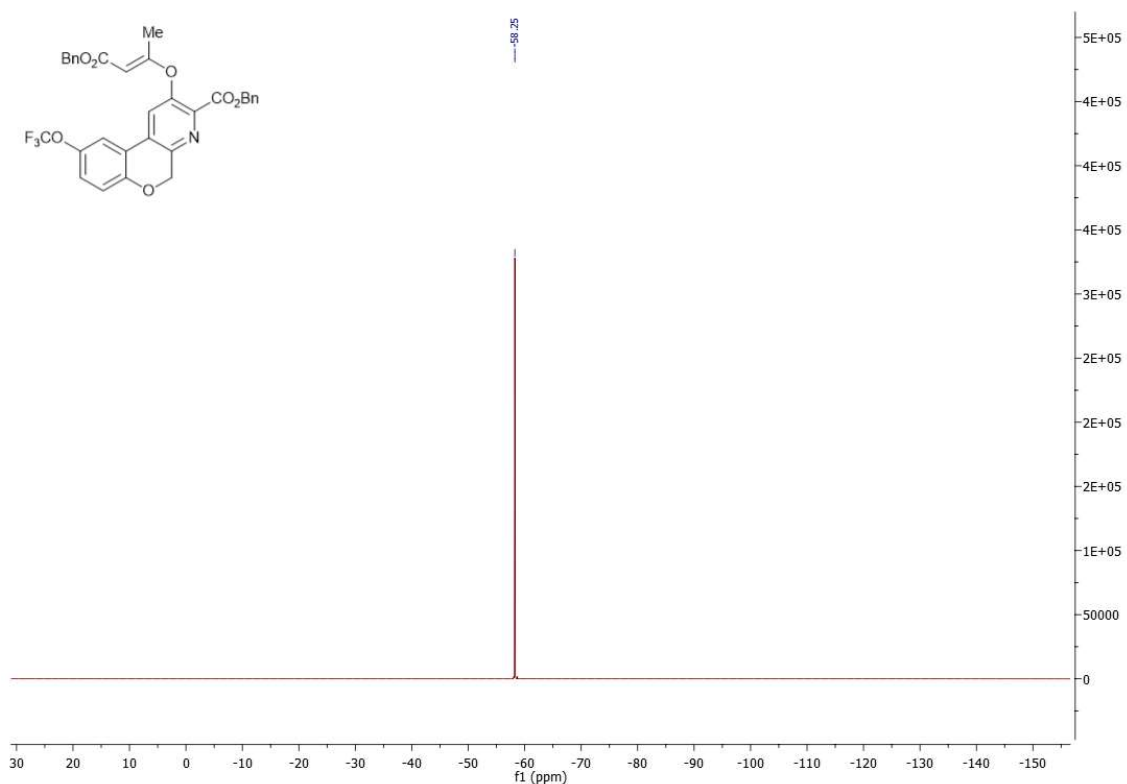


Figure S11b: ^{19}F NMR spectrum of compound **3h** (CDCl_3).

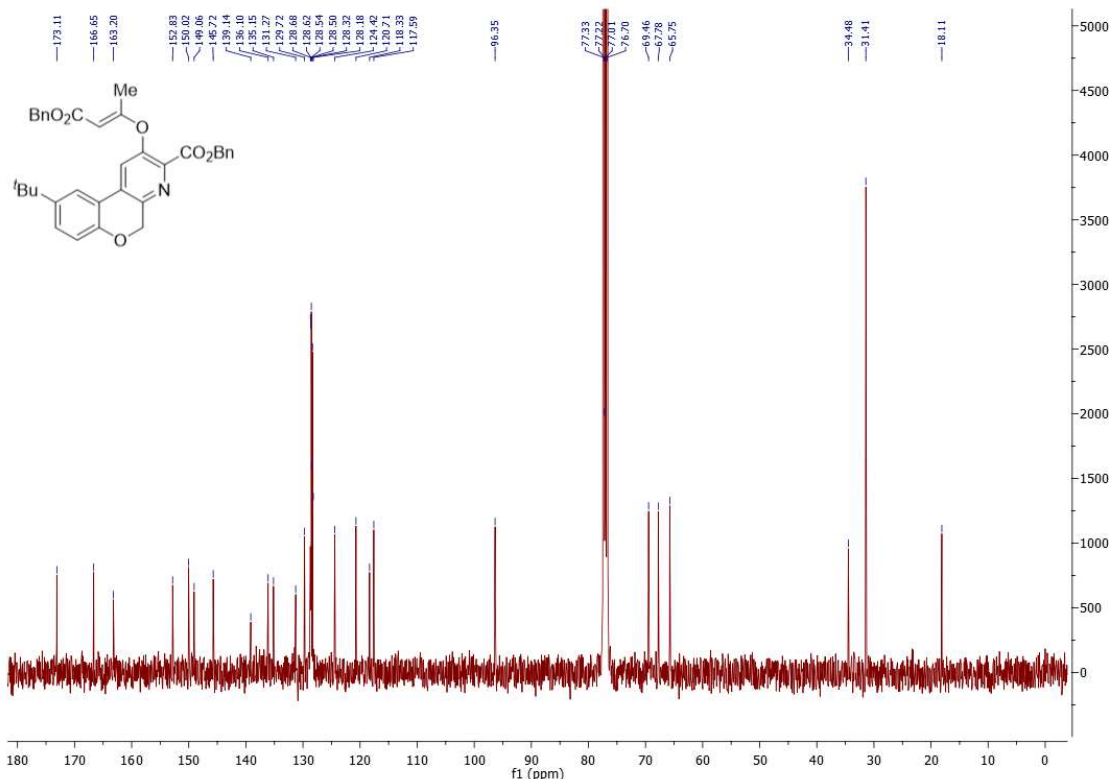
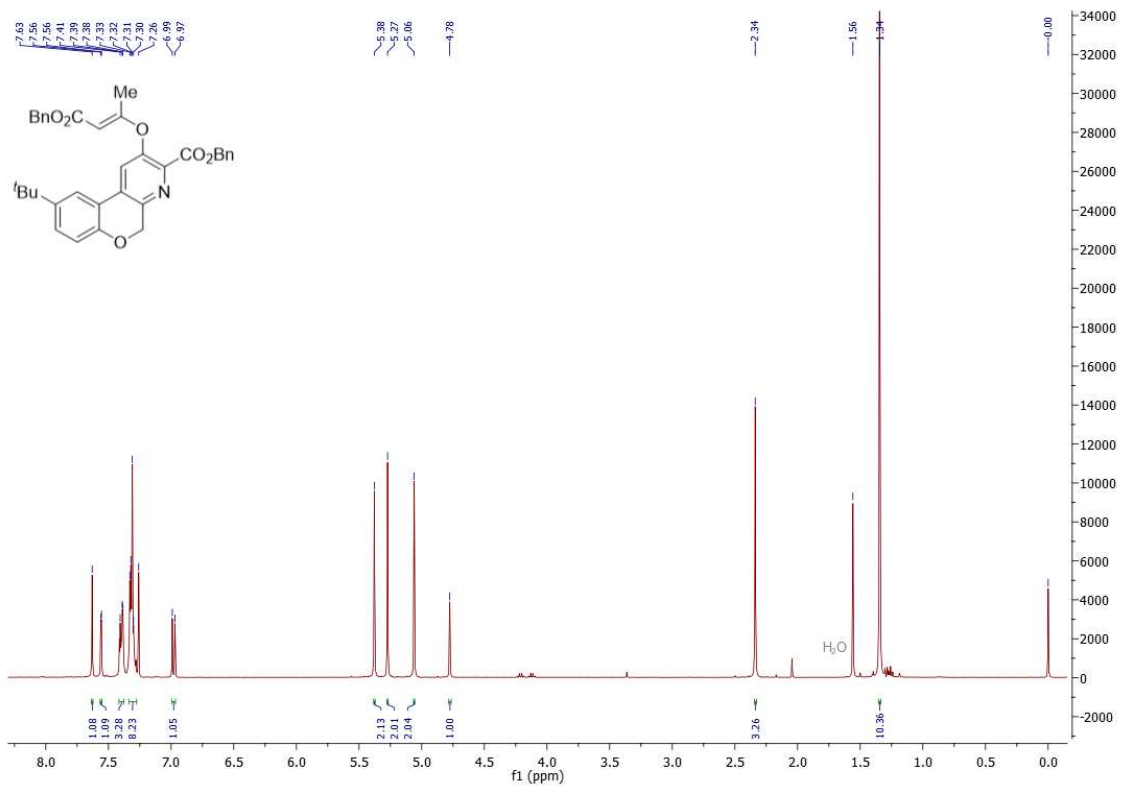


Figure S12: ¹H and ¹³C NMR spectra of compound 3i (CDCl₃).

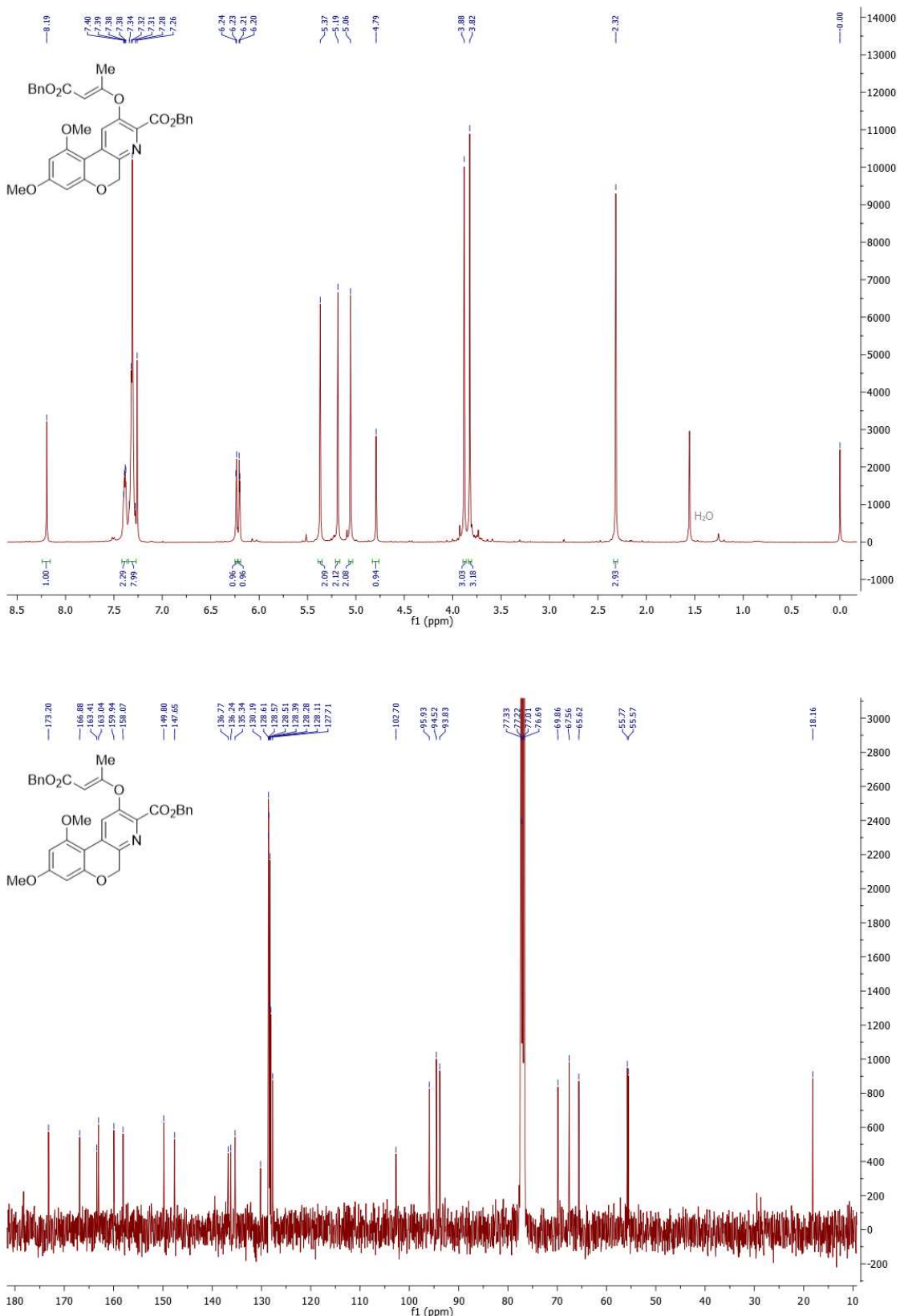


Figure S13: ^1H and ^{13}C NMR spectra of compound 3j (CDCl_3).

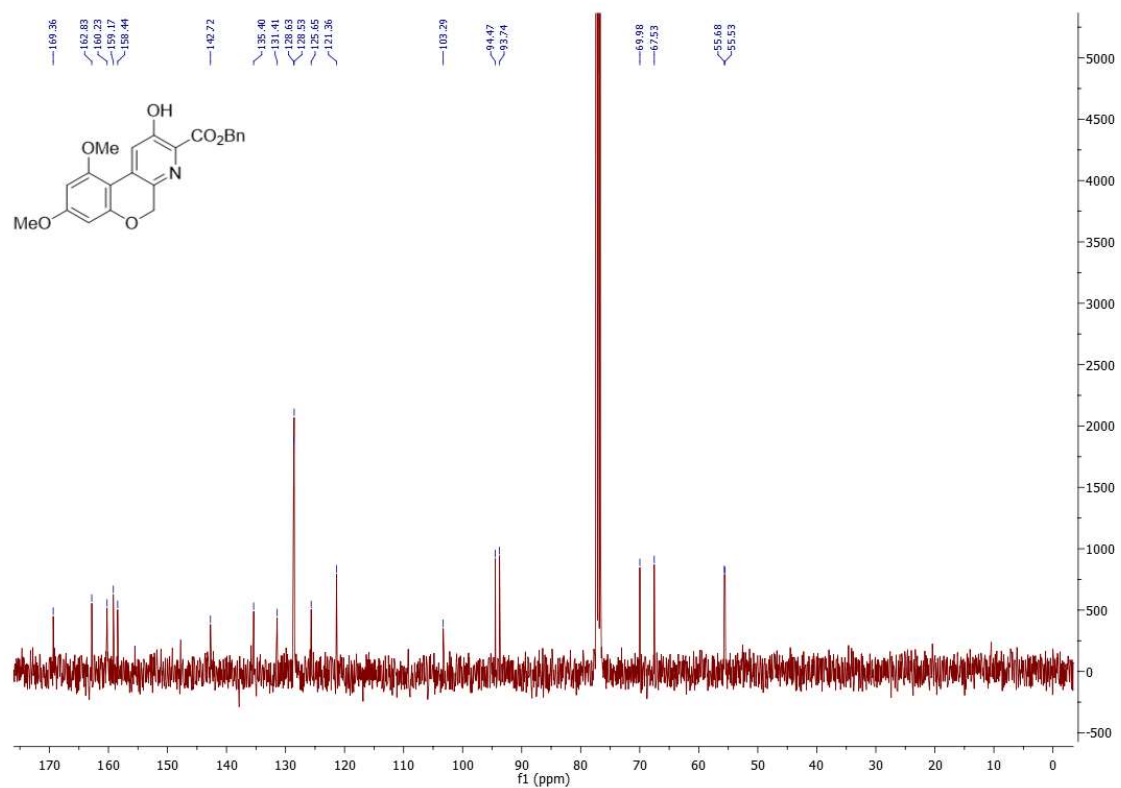
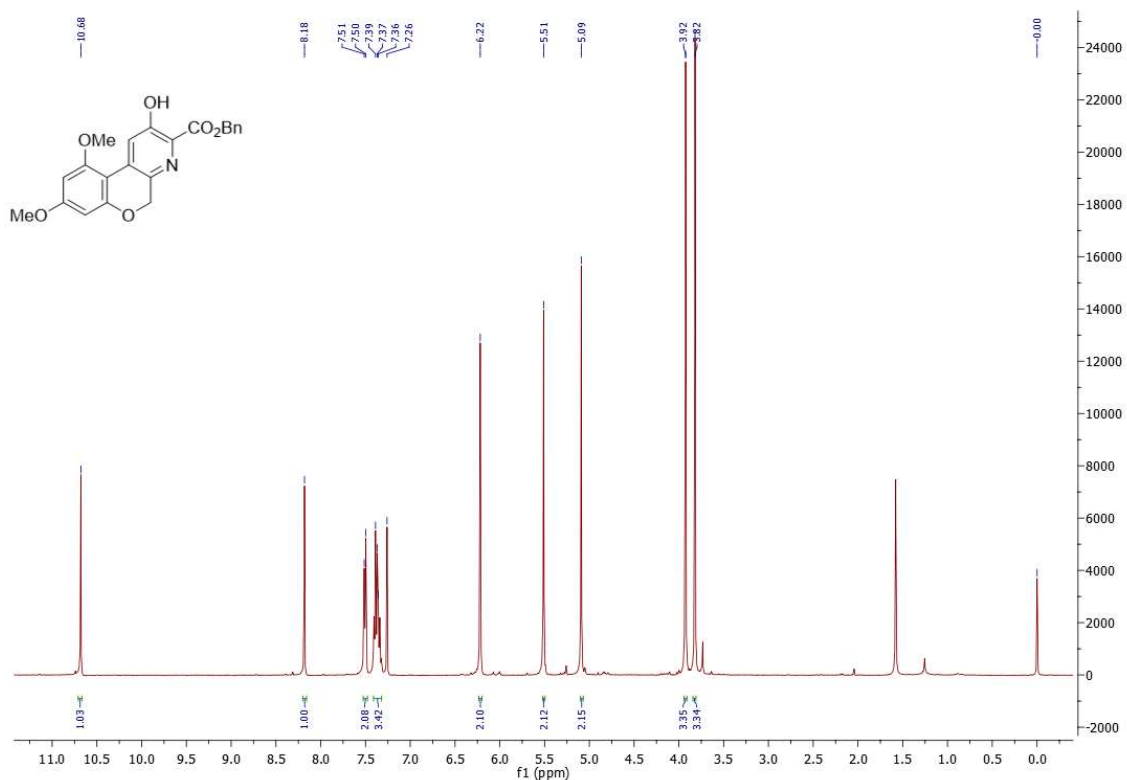


Figure S14: ^1H and ^{13}C NMR spectra of compound 4 (CDCl_3).

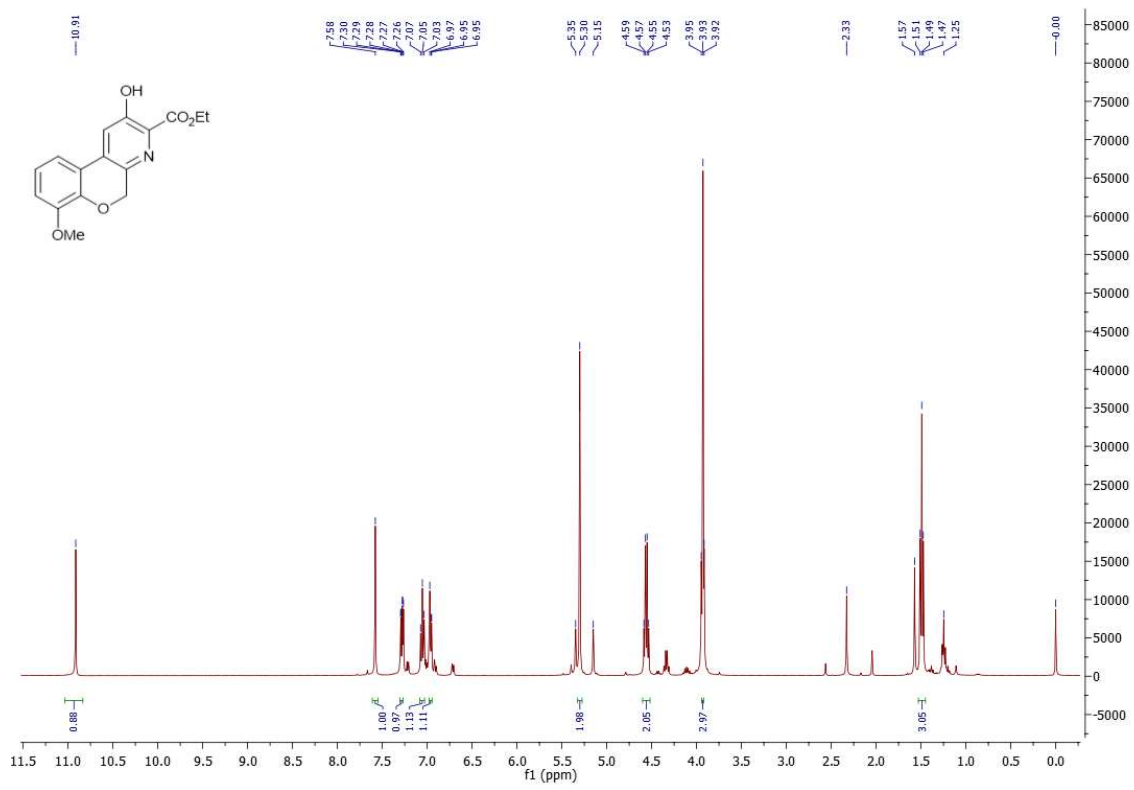


Figure S15: ^1H NMR spectrum of compound **6** (CDCl_3).

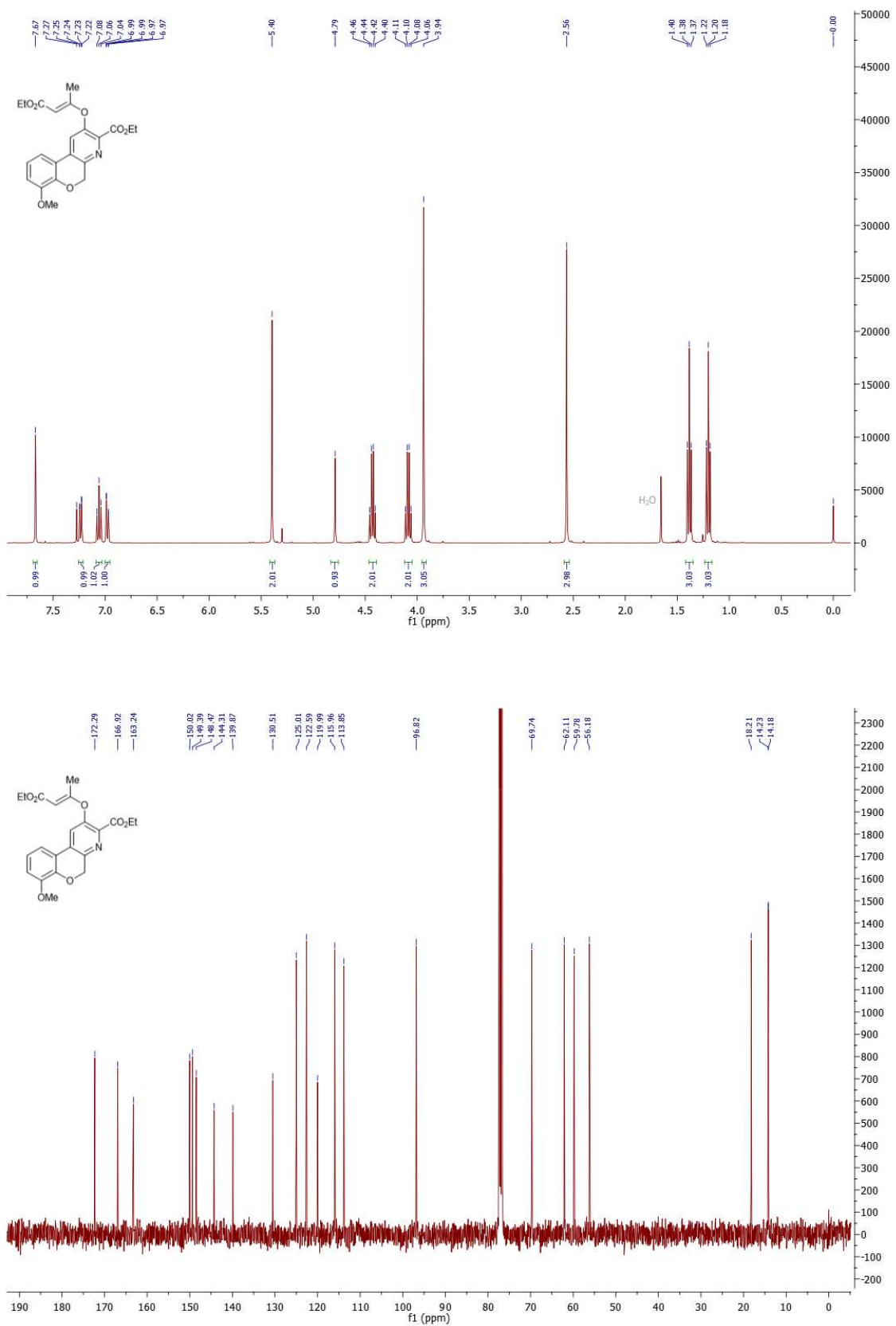


Figure S16a: ^1H and ^{13}C NMR spectra of compound **7** (CDCl_3).

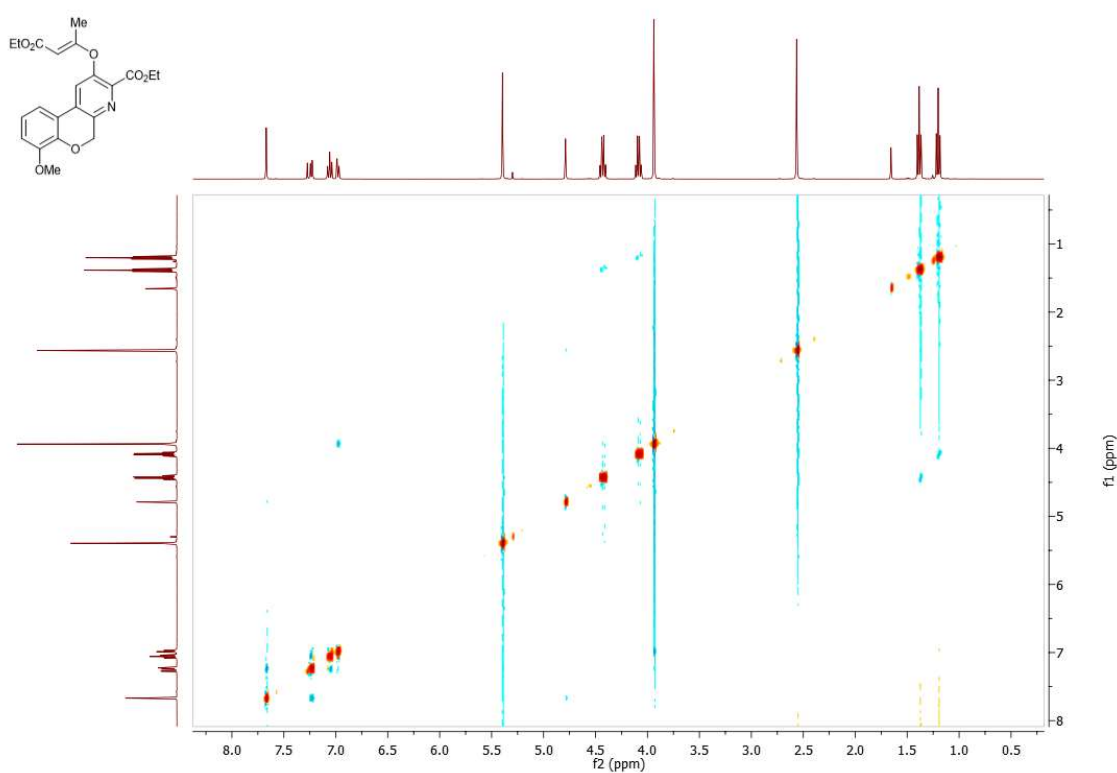


Figure S16b: NOESY spectrum of compound 7 (CDCl_3).

Crystallographic Data for Compounds **3b** and **4**

Table S1: Crystallographic data and details about refinement for structures **3b** and **4**.

	Compound 3b	Compound 4
Formula	$C_{33} H_{29} N O_7$	$C_{22} H_{19} N O_6$
M	551.57	393.38
λ (Å)	0.71073	0.71073
T (K)	296 (2)	296(2)
crystal system	Triclinic	Triclinic
space group	$P\ -1$	$P\ -1$
a (Å)	10.646(2)	8.708(2)
b (Å)	11.634(3)	13.624(4)
c (Å)	12.087(3)	17.004(5)
α (°)	101.823(13)	66.753(6)
β (°)	109.747(10)	79.781(7)
γ (°)	91.715(13)	88.762(7)
V (Å ³)	1371.0(6)	1821.5(9)
Z	2	4
ρ_{calc} (g.cm ⁻³)	1.336	1.434
μ (mm ⁻¹)	0.094	0.105
Crystal size	0.20 x 0.20 x 0.12	0.60 x 0.20 x 0.20
Crystal colour	Yellow	Yellow
Crystal description	Block	Prism
θ_{max} (°)	26.357	25.350
total data	33320	64553
unique data	5500	6676
R_{int}	0.1499	0.2185
R [$I > 2\sigma(I)$]	0.0422	0.0946
R_w	0.0985	0.1675
Goodness of fit	1.028	1.025
ρ_{min}	-0.655	-0.284
ρ_{max}	0.184	0.259

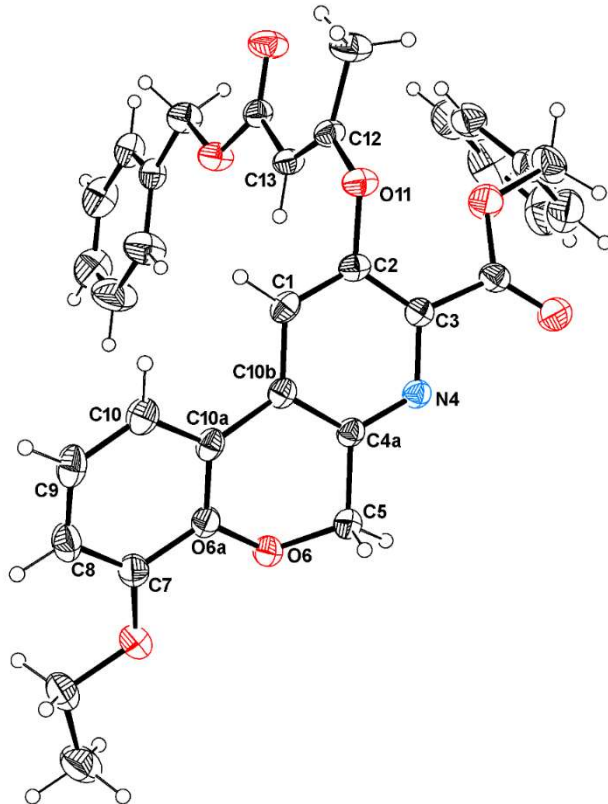


Figure S17. ORTEP-3 representation of compound **3b**, using 30% probability level ellipsoids (CCDC 2079932).

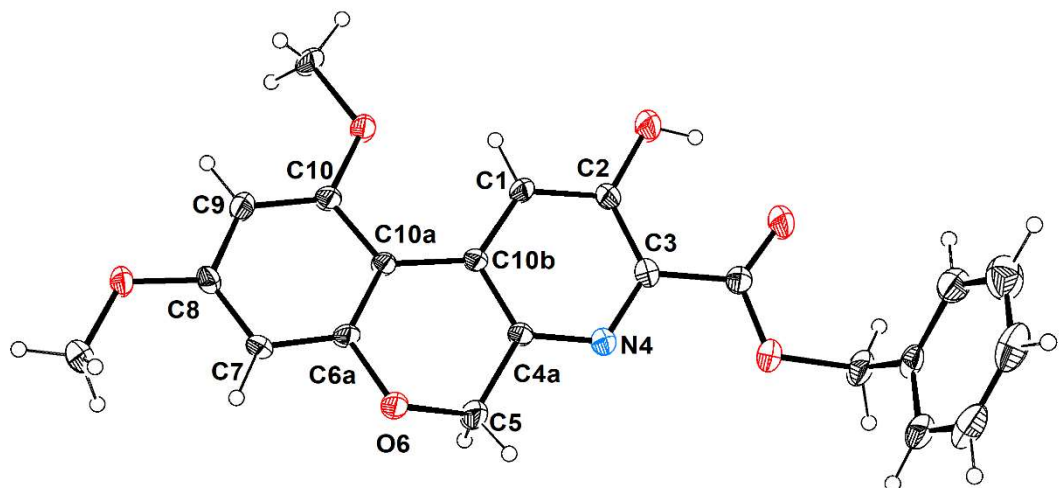
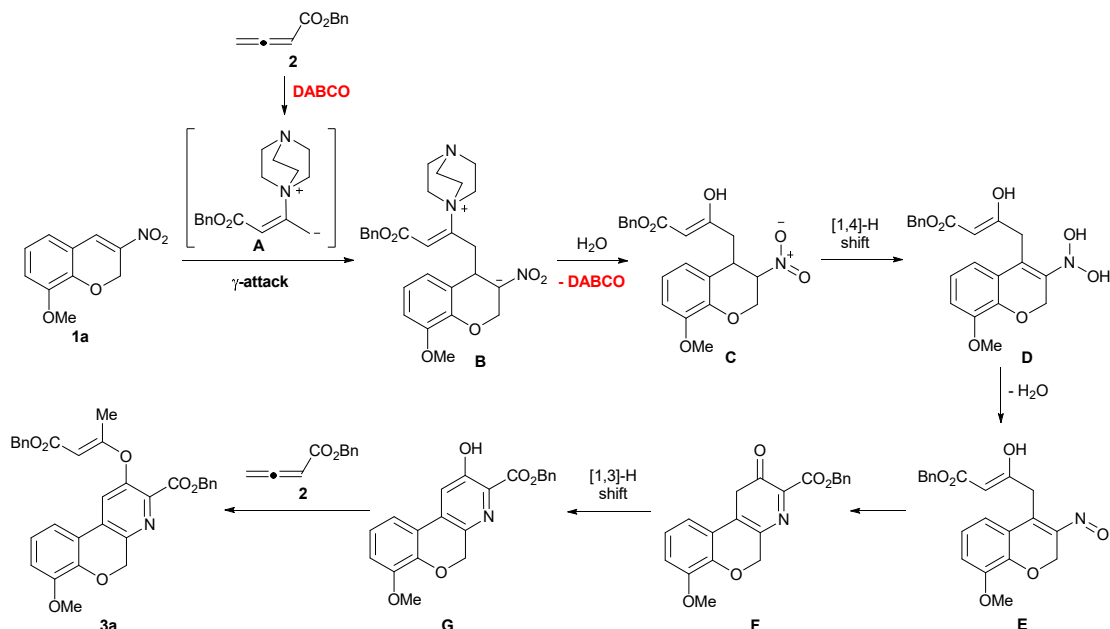


Figure S18. ORTEP-3 representation of compound **4**, using 30% probability level ellipsoids (CCDC 2079933).

Study of the Reaction Mechanism via Mass Spectrometry Analysis



Scheme S1. Proposed mechanism for the synthesis of 5*H*-chromeno[3,4-*b*]pyridines.

Table S2. Characterization of allene **2**, intermediates and final product **3a** by HRMS.

Compound		HRMS results				
Number/ Reference	Formula	Exact mass	Accurate mass	Ion formula	Exact mass	Err (ppm)
2	$\text{C}_{11}\text{H}_{10}\text{O}_2$	174.0681	175.0767	$\text{C}_{11}\text{H}_{11}\text{O}_2$	175.0765	-1.1
A	$\text{C}_{17}\text{H}_{22}\text{N}_2\text{O}_2$	286.1681	287.1764	$\text{C}_{17}\text{H}_{23}\text{N}_2\text{O}_2$	287.1754	-3.3
B	$\text{C}_{27}\text{H}_{31}\text{N}_3\text{O}_6$	493.2213	494.2300	$\text{C}_{27}\text{H}_{32}\text{N}_3\text{O}_6$	494.2286	-2.8
C/D	$\text{C}_{21}\text{H}_{21}\text{NO}_7$	399.1318	398.1243	$\text{C}_{21}\text{H}_{20}\text{NO}_7$	398.1245	+0.5
E	$\text{C}_{21}\text{H}_{19}\text{NO}_6$	381.1212	380.1136	$\text{C}_{21}\text{H}_{18}\text{NO}_6$	380.1140	+0.9
F/G	$\text{C}_{21}\text{H}_{17}\text{NO}_5$	363.1108	362.1046	$\text{C}_{21}\text{H}_{16}\text{NO}_5$	362.1034	-3.3
3a	$\text{C}_{32}\text{H}_{27}\text{NO}_7$	537.1788	576.1439	$\text{C}_{32}\text{H}_{27}\text{KNO}_7$	576.1419	-3.4

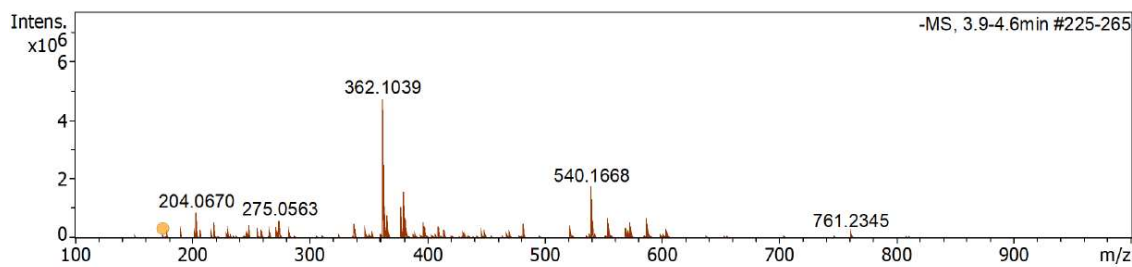


Figure S19. ESI(-)/HRMS spectrum of allene **2**.

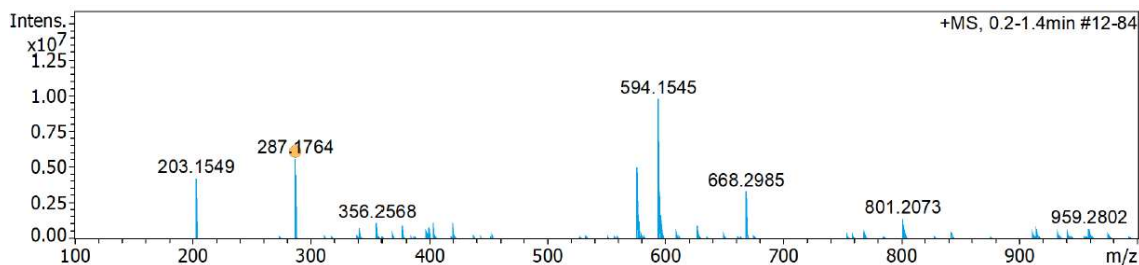


Figure S20. ESI(+)/HRMS spectrum of intermediate **A**.

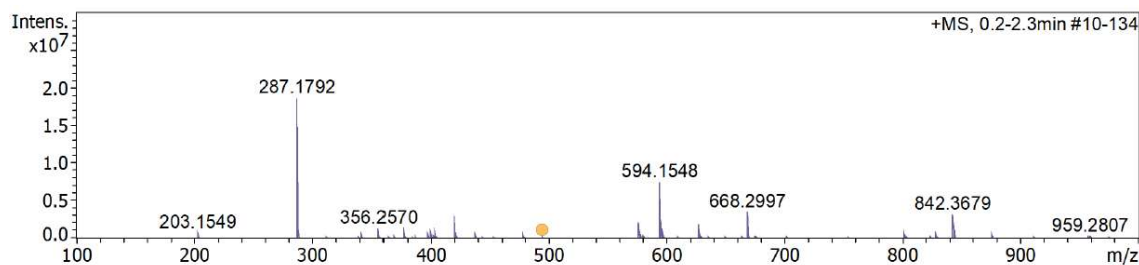


Figure S21. ESI(+)/HRMS spectrum of intermediate **B**.

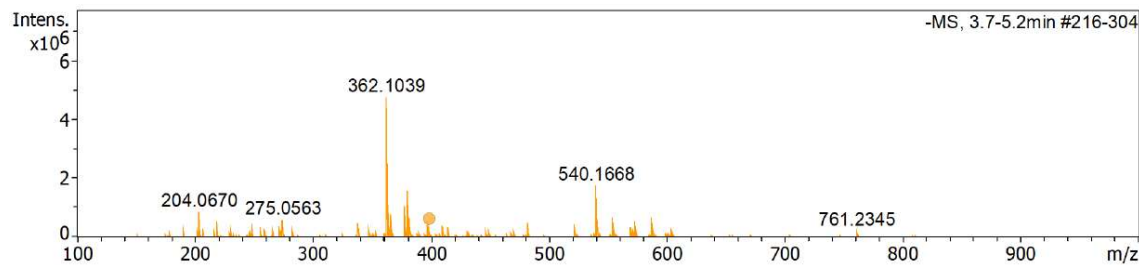


Figure S22. ESI(-)/HRMS spectrum of intermediate **C/D**.

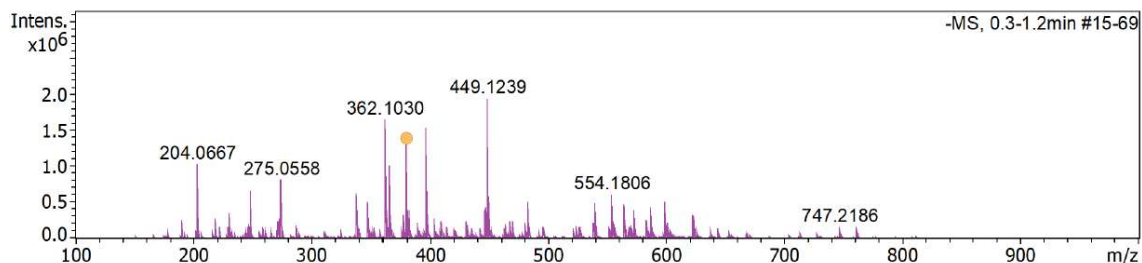


Figure S23. ESI(-)/HRMS spectrum of intermediate **E**.

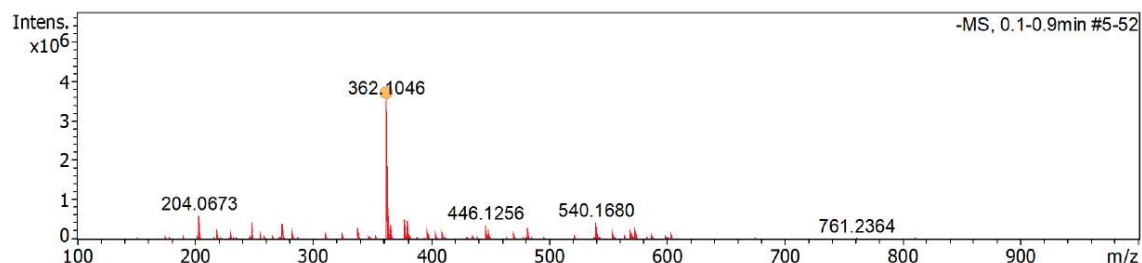


Figure S24. ESI(-)/HRMS spectrum of intermediate **F/G**.

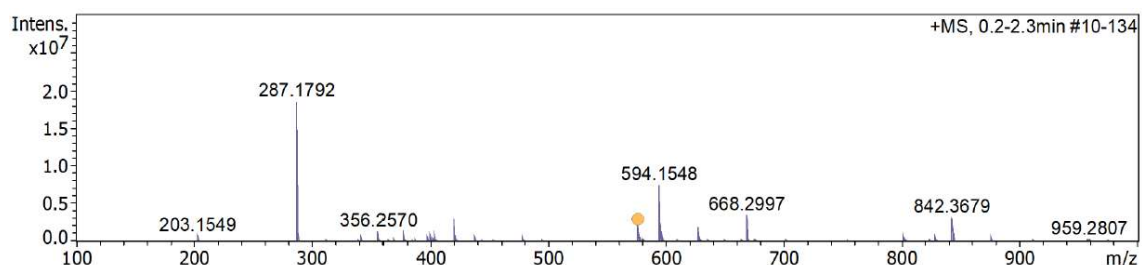


Figure S25. ESI(+)/HRMS spectrum of **3a**.

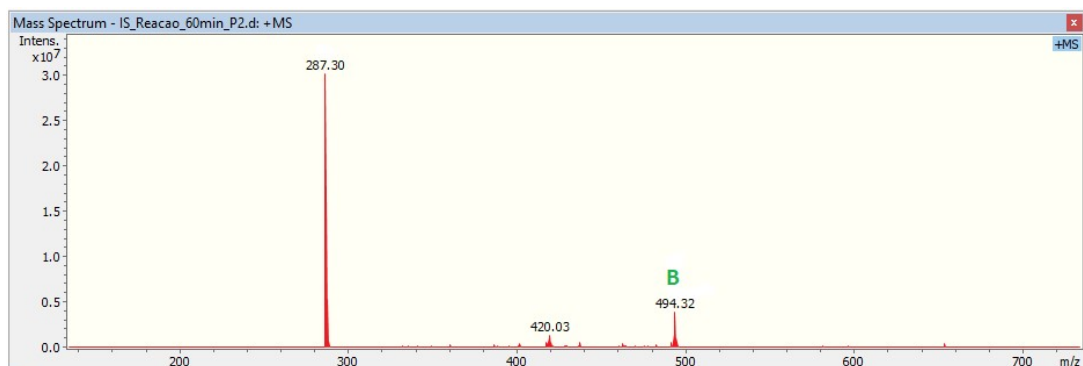


Figure S26. Full scan mass spectrum obtained in the ESI positive mode for the reactional mixture, at 60 min. The peak at m/z 494 was assigned to the protonated molecule of intermediate **B**. This precursor ion was isolated in the QIT mass analyser and CID experiments were done in order to obtain the MS^2 spectrum.

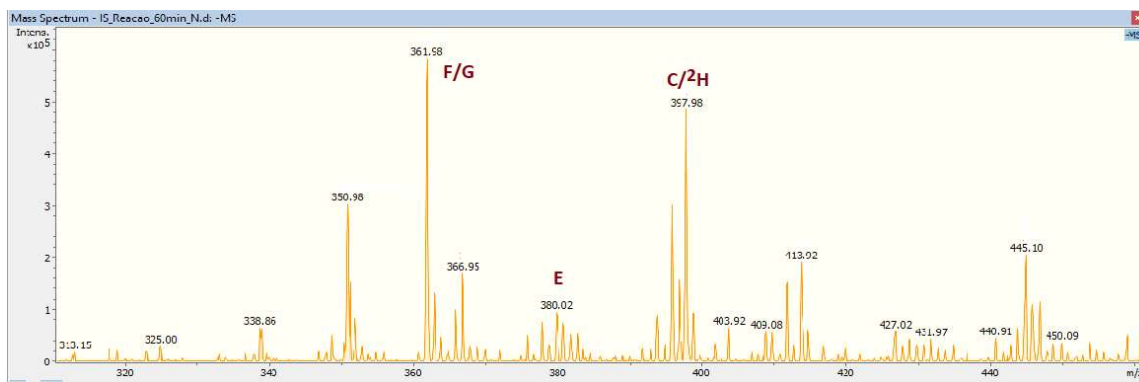


Figure S27. Full scan mass spectrum obtained in the ESI negative mode for the reactional mixture, at 60 min. The peaks at m/z 398, 380 and 362 were assigned to the deprotonated molecules of intermediates **C/D**, **E** and **F/G**, respectively. These precursor ions were isolated in the QIT analyser and CID experiments were performed in order to obtain the MS^2 spectra.

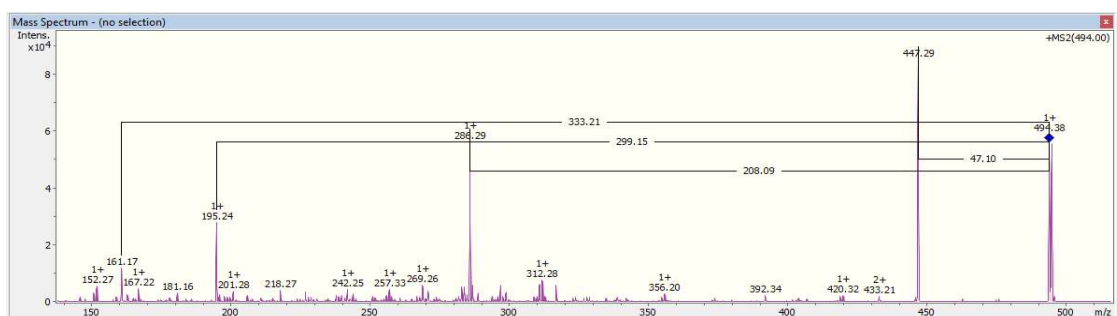


Figure S28. ESI(+)/ MS^2 spectrum of precursor ion m/z 494.

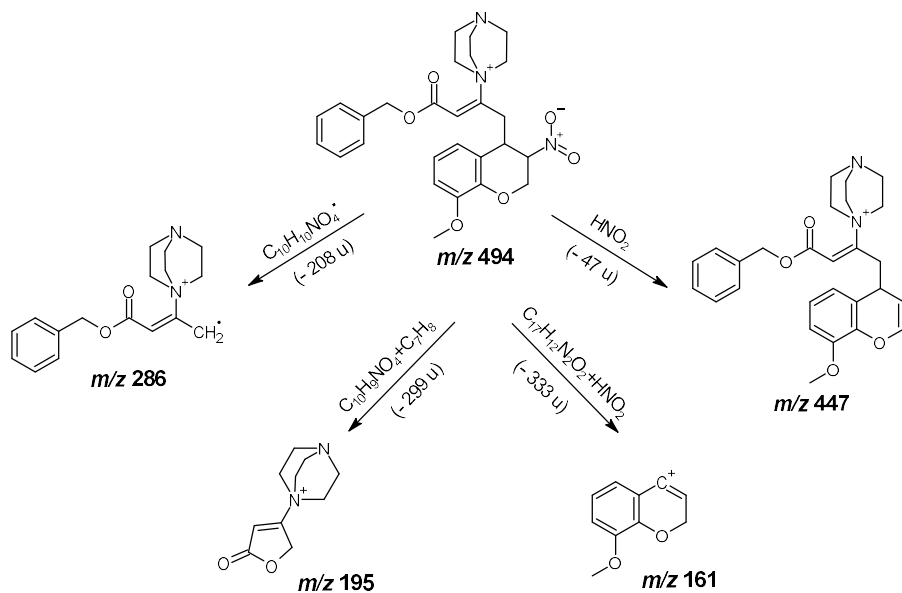


Figure S29. Proposed fragmentation patterns for the protonated molecule m/z 494 of intermediate **B**.

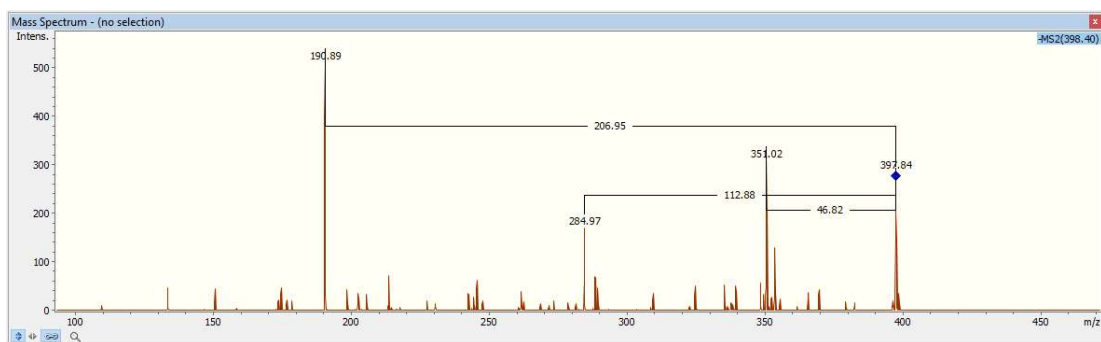


Figure S30. ESI(-)/MS² spectrum of precursor ion *m/z* 398.

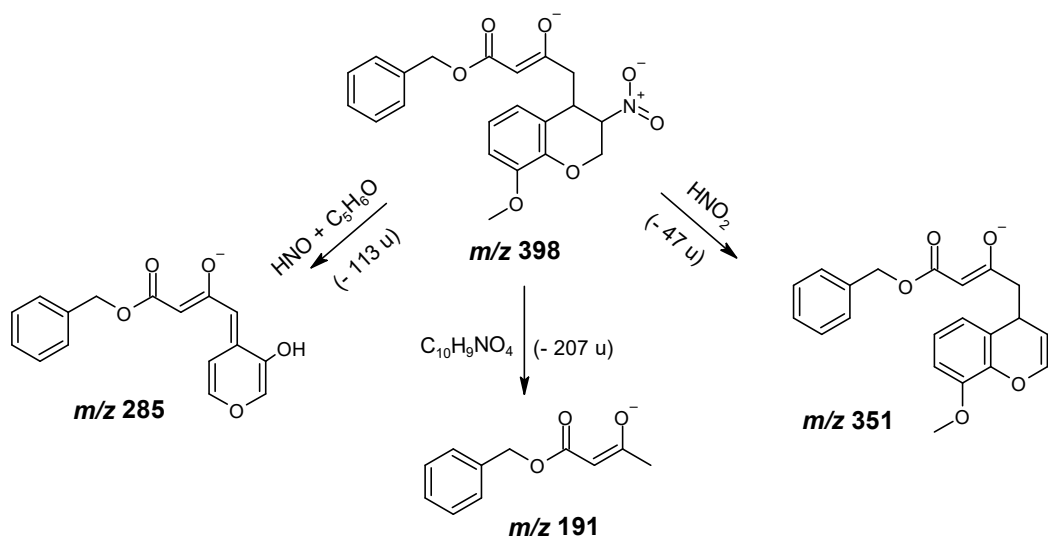


Figure S31. Proposed fragmentation patterns for the deprotonated molecule *m/z* 398 of intermediates C/D.

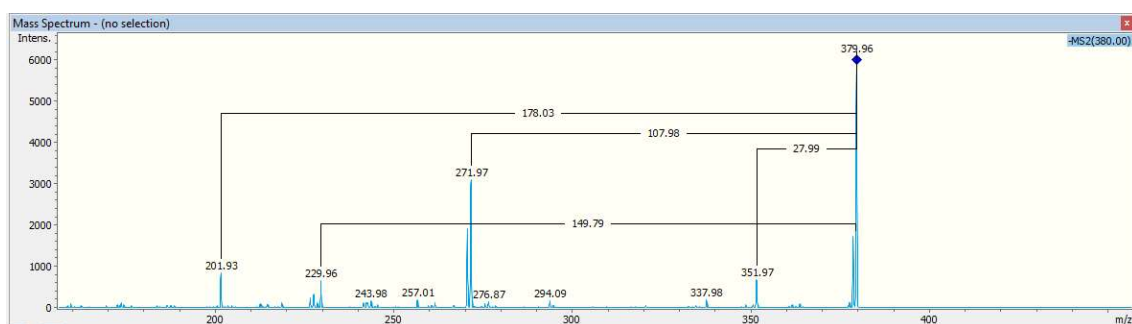


Figure S32. ESI(-)/MS² spectrum of precursor ion *m/z* 380.

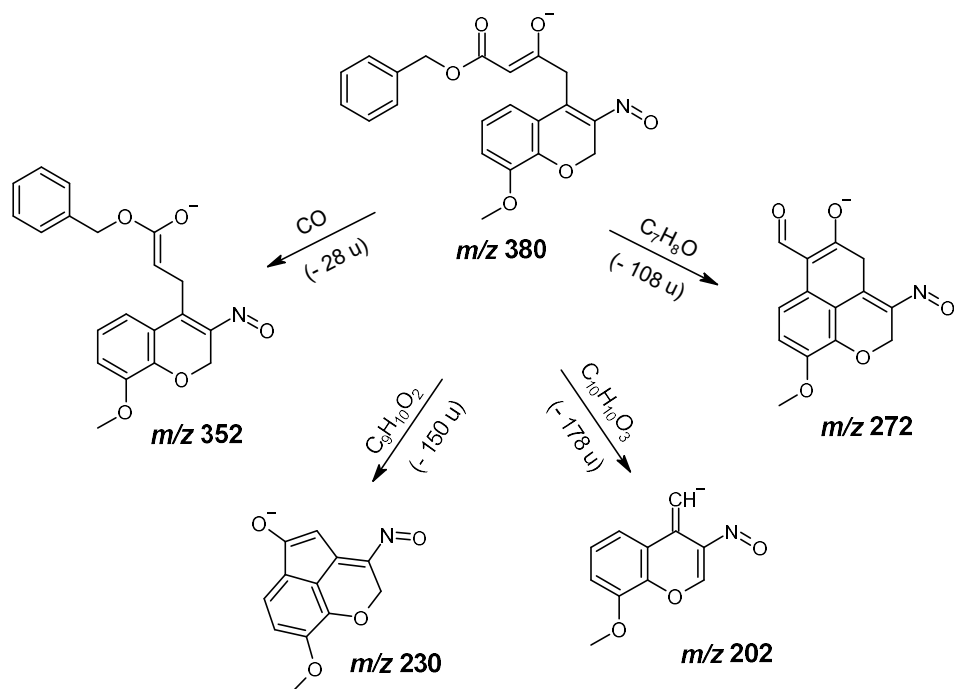


Figure S33. Proposed fragmentation patterns for the deprotonated molecule m/z 380 of intermediate **E**.

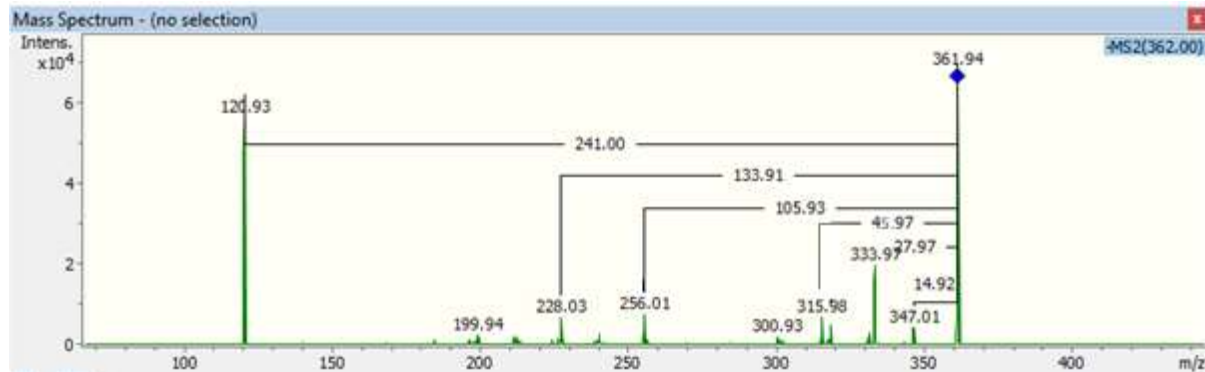


Figure S34. ESI(-)/MS² spectrum of precursor ion m/z 362.

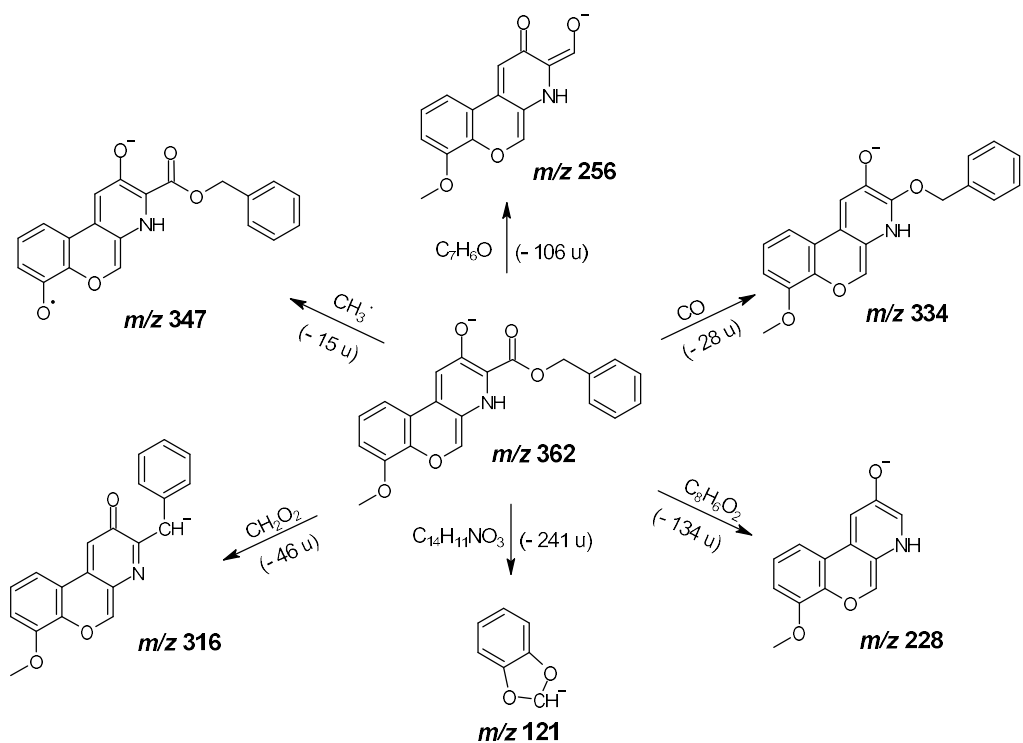


Figure S35. Proposed fragmentation patterns for the deprotonated molecule m/z 362 of intermediates **F/G**.